Reproductive Biology and Endocrinology

RESEARCH

Open Access

Bioengineered 3D ovarian model for long-term multiple development of preantral follicle: bridging the gap for poly(ε-caprolactone) (PCL)-based scaffold reproductive applications

Chiara Di Berardino[1*], Alessia Peserico[1], Chiara Camerano Spelta Rapini[1], Liliana Liverani[2,3], Giulia Capacchietti[1], Valentina Russo[1], Paolo Berardinelli[1], Irem Unalan[2], Andrada-Ioana Damian-Buda[2], Aldo R. Boccaccini[2] and Barbara Barboni[1]

Abstract

Background Assisted Reproductive Technologies (ARTs) have been validated in human and animal to solve reproductive problems such as infertility, aging, genetic selection/amplification and diseases. The persistent gap in ART biomedical applications lies in recapitulating the early stage of ovarian folliculogenesis, thus providing protocols to drive the large reserve of immature follicles towards the gonadotropin-dependent phase. Tissue engineering is becoming a concrete solution to potentially recapitulate ovarian structure, mostly relying on the use of autologous early follicles on natural or synthetic scaffolds. Based on these premises, the present study has been designed to validate the use of the ovarian bioinspired patterned electrospun fibrous scaffolds fabricated with poly(ε-caprolactone) (PCL) for multiple preantral (PA) follicle development.

Methods PA follicles isolated from lamb ovaries were cultured on PCL scaffold adopting a validated single-follicle protocol (Ctrl) or simulating a multiple-follicle condition by reproducing an artificial ovary engrafted with 5 or 10 PA (AO_{5PA} and AO_{10PA}). The incubations were protracted for 14 and 18 days before assessing scaffold-based microenvironment suitability to assist in vitro folliculogenesis (*iv*F) and oogenesis at morphological and functional level.

Results The *iv*F outcomes demonstrated that PCL-scaffolds generate an appropriate biomimetic ovarian microenvironment supporting the transition of multiple PA follicles towards early antral (EA) stage by supporting follicle growth and steroidogenic activation. PCL-multiple bioengineering *iv*F (AO_{10PA}) performed in long term generated, in addition, the greatest percentage of highly specialized gametes by enhancing meiotic competence, large chromatin remodeling and parthenogenetic developmental competence.

*Correspondence:
Chiara Di Berardino
cdiberardino@unite.it

Full list of author information is available at the end of the article

Conclusions The study showcased the proof of concept for a next-generation ART use of PCL-patterned scaffold aimed to generate transplantable artificial ovary engrafted with autologous early-stage follicles or to advance *iv*F technologies holding a 3D bioinspired matrix promoting a physiological long-term multiple PA follicle protocol.

Keywords PCL-electrospun scaffold, in vitro folliculogenesis, in vitro oogenesis, Tissue engineering, Artificial-ovary, Preantral follicle development, Oocyte maturation, Large chromatin remodeling, Parthenogenetic activation, Embryo development

Background

Assisted Reproductive Technologies (ARTs) have a consolidated role in human and animal reproductive management [1]. Although in humans they are intended to overcome infertility or prevent genetically transmissible diseases, in veterinary medicine, they are primarily directed towards financial purposes or biomedical research [2]. The most standardized ARTs are the in vitro oocyte maturation (IVM), fertilization (IVF), and embryo culture technologies, collectively termed embryo production.

Nevertheless, effectively managing early folliculogenesis and oogenesis remains an unresolved challenge in ART, constraining the ability to rejuvenate reproductive endocrine control and optimize the availability of fertilizable female gametes, while leveraging the extensive untapped reserve represented by immature oocytes. In this context, in vitro folliculogenesis (*iv*F) and ovarian transplantation are the most promising technologies [3–9] in order to face either human fertility in case of premature reduction of female gamete reserve (young oncological patients and premature menopause) or animal reproduction to enhance the reproductive performance of highly selected domestic mammals or to preserve biodiversity by contrasting the reduced numerical strength of mammalian endangered species [10–15].

The transplantation of cryopreserved ovarian tissue is promising for restoring reproductive functionality, but it is limited by the risk of transferring tumor cells. A potential strategy is to use artificial ovaries made from engineered biomaterials, which can be populated with follicles in early development stages and have robust survival rates after cryopreservation treatment. The reproductive research sector is focusing on innovative platforms using three-dimensional (3D) artificial environments to overcome these limitations [16–27].

3D technologies are being used to engineer female biomimetic reproductive tissues, generating integrated multi-organ in vitro systems. These systems involve different cell compartments controlling female reproductive homeostasis and function, resulting in a complex paracrine mechanism controlling reproductive outcomes. This approach is a backward path to the origin of ARTs and is now being applied to Reproductive Tissue Engineering (REPROTEN) in various fields of investigative biology and medicine [18, 28, 29]. In particular, REPROTEN is based on the availability of tissue-specific materials, that have to be engineered to mimic the reproductive environments. This multifaceted approach, offering a potential therapeutic avenue for tumor treatment, underscores the transformative potential of the REPROTEN paradigm in complex clinical scenarios [17, 30]. To build up a bioengineered artificial ovary replicating the intricate native ovarian system, biocompatible scaffolds encapsulating isolated follicles and/or autologous ovarian cells are required [31].

Scaffolds fulfilling and replicating the reproductive matrix requirements are currently available by taking advantage of either the specific derived-natural tissue matrixes and synthetic polymers or emerging fabrication techniques.

In the landscape of artificial ovary construction, various materials, including ovarian decellularized bio-scaffolds [27, 32], alginate matrix [33, 34], fibrin gel [35–37], PEG hydrogel [38], and gelatin-based 3D-printed scaffolds [39], have been proposed in rodent models [31].

Amongst the emerging fabrication techniques laser cut manufacturing technique, in which a continuous wave laser is used to process materials with very high precision, has been frequently used. Templates for the cutting process can be generated by computer-aided design (CAD) [39–42]. Thus, the manufacturing process is highly flexible and replicable with respect to the final design of a generated sheet and the resulting 3D scaffold [43].

Three- and four-dimensional printing are essential tools for fabricating biomimetic scaffolds, using additive manufacturing techniques to achieve predefined shapes and controlled spatial chemistry and geometry. This involves using 3D software to create a model, which is then imported into slicing software and printed using a 3D printer. Four-dimensional printing, an advanced version, uses smart materials to mimic the dynamic nature of tissues to a very large extent [29, 39, 40, 42–47].

Electrospinning pursues a biomimetic approach in the scaffold design [48, 49] by generating nano- and microfibers mimicking the native extracellular matrix (ECM) morphology and these fibers can be easily functionalized with active biomolecules (i.e. drugs, growth factors, proteins, etc.). Recently, the scaffold-based tissue engineering approach started to be applied to the fabrication of ovarian stroma. A relevant novelty in the field [50] is the

fabrication of 3D printing and electrospun patterned constructs which are able to support the development of ovarian follicles [39, 51–53].

Recent results demonstrated that poly(ε-caprolactone) (PCL), an FDA-approved material often used as an implantable material in the human body, can be exploited to fabricate bioinspired matrices for ovarian stroma, compatible with long-term ovarian follicle survival [51, 52, 54, 55].

The ovarian bioinspired PCL-patterned scaffolds have been recently used to perform 3D *iv*F of single preantral (PA) follicles protocols [56] to reproduce the gonadotropin-sensitive phase of transition to early antral (EA). This sets the stage for subsequent in vivo selection by gonadotropins during the EA phase, highlighting its potential in mimicking natural follicular development [57, 58].

While PCL exhibits promise, demonstrating its capability to support the simultaneous survival and development of multiple follicles remains a critical challenge. This is a crucial step in proving its suitability for constructing an artificial ovary that can effectively mimic the natural follicular environment once transplanted.

To this aim, the present research has been designed to collect the proof of concept of the innovative patterned electrospun fibrous scaffolds produced by "green electrospinning" [52] in generating functional artificial ovaries by testing them in vitro on a multiple 3D *iv*F system designed using mechanically isolated prepubertal sheep preantral follicles. This approach, driving innovation, harmonizes into the biomimetic environment the sequential processes of ovarian follicle recruitment during the transition from PA to EA by mimicking a key reproductive step of folliculogenesis (transition from gonadotropin responsive to gonadotropin-dependent follicular phase) and oogenesis (acquisition of oocyte meiotic competence) [58]. The experimental plan was set up to compare the somatic and germinal compartment outcomes after a 14 days (validated protocol) or long-term (18 days) 3D incubation performed on PCL scaffold engineered with single [56] or multiple PA follicles. This latter model has been designed to reproduce an artificial ovary enriched with 5 (AO_{5PA}) or 10 PA (AO_{10PA}) follicles. The morphological and functional assessments provide crucial insights into the biomimicry of patterned electrospun fibrous scaffold [59–63], which enabled long-term follicle development (survival, growth, antrum differentiation) and oocyte specialization (large chromatin remodeling and acquisition of both meiotic and partial developmental competence).

Altogether, the results established with strong functional in vitro evidence of the long-term biocompatibility of patterned electrospun fibrous scaffolds fabricated with PCL, an FDA-approved biomaterial, thus represents a significant stride toward its conceivable future use in costuming engineered artificial ovary to be transplanted or for advancing the *iv*F protocols, underscoring the transformative potential of Tissue Engineering approaches in reproductive medicine.

Materials and methods

Chemicals

All chemicals used in this study were purchased from Sigma (Sigma Chemical Co., St. Louis, MO, USA) unless otherwise specified.

Ethic issues

No ethical issues were encountered in the present research, as all biological materials were obtained from tissues of animals in the food chain discarded by the local slaughterhouse.

Biological sample recovery

Ovaries collection

The primary objective of this study was to conduct in vitro follicle growth of PA follicles isolated from the ovaries of Appenninica breed sheep lambs obtained from animals intended for consumption [64]. A total of twelve ewes, each approximately 5 months old, contributed 24 ovaries for this investigation.

The ovaries were swiftly transported to the laboratory in a thermostatic container, maintaining a temperature of 38 °C during the transportation from the slaughterhouse, and arrived within one hour. Upon arrival, the ovaries underwent a thorough rinse in NaCl 0.9% solution supplemented with benzoxonium chloride 1 mg/mL (Cat. No. 032186013 Bialcol Med, Vemedia Pharma S.r.l., Parma, Italy) prior to any manipulations.

Following the removal of the medulla, the ovaries were transferred into HEPES-buffered TCM199 medium (Cat. No. M7528, Sigma) and meticulously dissected into cortical strips measuring 0.5×0.5×0.5 cm.

Isolation, morphological evaluation, and in vitro culture of PA follicles

PA follicles were mechanically isolated from cortical strips using 32 G sterile needles under a stereomicroscope within a flow hood to prevent damage to the theca layer. Selection criteria were based on morphology and size [65]. The medium-large PA follicles utilized for in vitro culture experiments exhibited an average diameter of 245±5 µm. This specific category, known for its superior in vitro growth performance [65–67], was identified using an inverted-phase microscope and the time-lapse imaging software NIS-Elements (Eclipse Ti Series, Nikon, Tokyo, Japan) to determine the PA diameter.

This meticulous selection process facilitated the exclusion of follicles with damaged basal membranes, while those displaying early signs of degeneration were

discarded (follicles lacking follicular 3D microarchitecture, featuring oocyte extrusion, and exhibiting a darkened appearance in the somatic compartment). According to the experimental groups, the culture was conducted for 14 and 18 days at 38.5 °C and 5% CO_2 in Minimum Essential Medium α (aMEM; Cat. No. BE02-002 F Lonza, Basel, Switzerland) supplemented with 5% Knockout™ Serum Replacement (Knockout™ SR; Cat. No. 10,828,028 Gibco, Thermo Fisher Scientific, Waltham, MA, USA), 1% ITS (insulin, transferrin, and selenium; Cat. No. I1884, Sigma), 50 µg/mL of ascorbic acid (Cat. No. A4544, Sigma), 2 mM of glutamine (Cat. No. BE17-605E/U1 Lonza), and antibiotics (75 mg/L of penicillin-G, 50 mg/L of streptomycin sulfate; Cat. No. DE17-602E Lonza) [56, 64].

For the single-PA follicle in vitro culture (Ctrl group), the trans-well systems were filled with 100 µL of *iv*F culture medium. For multiple-PA follicles in vitro culture, the trans-well systems were filled with 100 µL (Artifical Ovary/AO_{5PA} group) and 233 µL (AO_{10PA} group) of *iv*F culture medium, according to the experimental groups. For multiple-follicles in vitro culture, the correct numerical (5 or 10 PA/well) and volumetric (µL) ratio per well has been maintained according to the trans-well culture system adopted.

The culture medium was changed every 48 h and supplemented with 4 IU/mL of equine Chorionic Gonadotropin (eCG; equivalent to 1 µg/mL FOLLIGON®, MSD Animal Health S.r.l., Segrate, Italy), as previously validated [56, 57, 64]. The eCG's biological activity was declared to be 5000 IU per vial in accordance with the manufacturer's instructions.

in vitro PA follicles culture protocols comparison

The medium-large PA follicles used for the in vitro culture experiments showed a mean diameter of 245±5 µm. The healthy medium-large PA follicles were randomly assigned to different culture *iv*F protocols, and the procedure was carried out by adopting single-follicle (Ctrl) and multiple-follicle (AO) approaches (Fig. 1). The electrospun fibrous morphology and scaffold topology confirmed the formation of a pattern with macropores averaging 300 µm in size, along with an average fiber diameter of approximately 1 µm [52, 56, 58, 62]. Consequently, PA follicles are housed within these culture macropores formed by the alignment of fibers. More in detail: (A) single-follicle validated approach designed by carrying out the whole PA follicle culture on the trans-well culture system with PCL-patterned scaffold that fits into a 96-well plate U-shaped (Ctrl) [56]; (B) multiple-follicles approach (5 PA x well) designed by carrying out

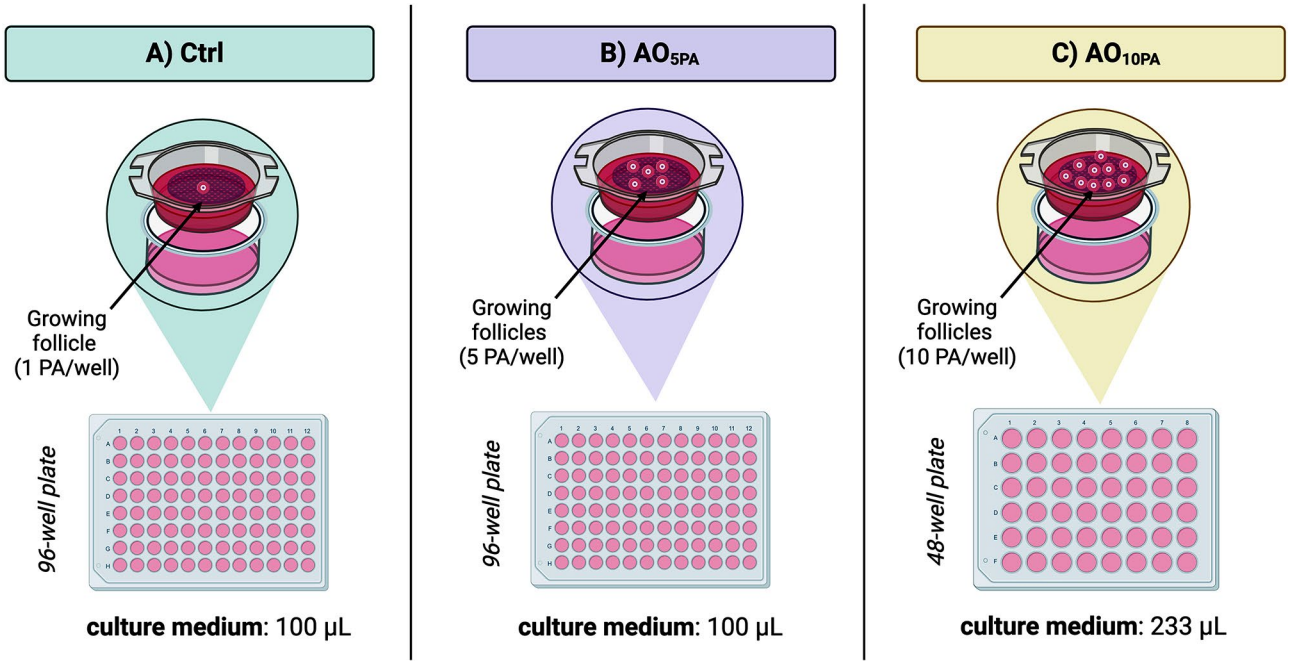

Fig. 1 *iv*F culture protocols carried out on single (**A**) and multiple-follicle approaches (**B**, **C**). The electrospun fibrous morphology and scaffold topology confirmed the formation of a pattern with macropores averaging 300 µm in size, along with an average fiber diameter of approximately 1 µm [52, 56, 58, 62]. Consequently, PA follicles are housed within these culture macropores formed by the alignment of fibers. More in detail: (**A**) single-follicle validated approach designed by carrying out the whole PA follicle culture on the trans-well culture system with PCL-patterned scaffold that fits into a 96-well plate U-shaped (Ctrl) [56]; (**B**) multiple-follicles approach (5 PA x well) designed by carrying out the whole PA follicle culture on trans-well culture system with PCL-patterned scaffold that fits into a 96-well plate U-shaped (AO_{5PA}); (**C**) multiple-follicles approach (10 PA x well) designed by carrying out the whole PA follicle culture on trans-well culture system with PCL-patterned scaffold that fits into a 48-well plate U-shaped (AO_{10PA}). Created with Biorender.com

the whole PA follicle culture on trans-well culture system with PCL-patterned scaffold that fits into a 96-well plate U-shaped (AO_{5PA}); (C) multiple-follicles approach (10 PA x well) designed by carrying out the whole PA follicle culture on trans-well culture system with PCL-patterned scaffold that fits into a 48-well plate U-shaped (AO_{10PA}).

For multiple-follicles in vitro culture, the correct numerical (5 or 10 PA) and volumetric (µL) ratio per well has been maintained according to the trans-well culture system adopted.

Three independent biological replicates were performed for each tested protocol, comparing the performances of *iv*F by assessing the morphological and functional analysis of the in vitro follicle development and meiotic competence acquisition of in vitro follicle-grown oocytes.

in vitro PA follicles culture outcomes

Morphological and functional analysis of in vitro follicle development

The *iv*F outcomes at the end of the long-term culture (14 and 18 days) were defined by considering follicle growth, antral cavity differentiation, and the incidence of degeneration.

The in vitro follicle growth was analyzed by recording the final diameters detected using an inverted microscope (time-lapse imaging software NIS-Elements, Eclipse Ti Series, Nikon, Japan) and expressed as the rate of increasing size (Δ growth %).

The degenerated follicles that had lost the 3D microarchitecture, extruded the oocytes, and/or displayed a darkened aspect of the somatic compartment were discarded.

On the contrary, the following analyses collected the healthy follicles classified as having either "no antrum" or "early antral" (EA) structures based on the follicular 3D microarchitecture with a translucent oocyte and follicular cells with the absence or presence of a preliminary follicular cavity (antrum). Small antral (SA) follicles, serving as the gold standard of reference, are characterized by their larger size (approximately 500 µm in diameter), more developed morphology (exhibiting well-defined antral cavities and multiple layers of granulosa cells), and a more advanced stage of functional capacity, compared to the smaller and less mature early antral follicles.

Maturation of follicle enclosed oocyte (FEO) derived from EA follicles in vitro

At the end of the *iv*F, the obtained in vitro grown EA follicles displayed a mean diameter of 380±9 µm. The gained EA follicles were accurately analyzed under an inverted-phase microscope associated with the time-lapse imaging software, NIS-Elements Advanced Research software 4.51.00 (Eclipse Ti Series, Nikon Europe BV, Amsterdam, The Netherlands), to determine its diameter and to exclude any morphological signs of degeneration such as somatic cell or oocyte darkness, loss of compactness of granulosa layer or basal membrane break.

The selected EA follicles were matured according to experimental groups on our previously validated FEO approach [58], using 96- and 48-well plates with U-shaped wells and with the holder filled with PCL-patterned electrospun scaffolds.

The whole EA follicles were incubated on confluent monolayers of ovarian surface epithelium (OSE) cells. More in detail, OSE cells, previously validated by our group as cell monolayer coculture [56, 58, 64], were isolated using a surgical scalpel from the ovarian cortex of pre-pubertal ovaries previously incubated in 0.25% Trypsin/EDTA 200 mg/L at 38.5 °C for 5 min. Cell suspensions were collected into a petri dish (6 cm), filled with Dulbecco's Phosphate Buffered Saline (DPBS; Cat. No. D8662, Sigma) solution containing 30% Fetal Bovine Serum (FBS; Cat. No. 11,573,397, Gibco, Darmstadt, Germany) to inactivate Trypsin, centrifuged, and the supernatant discarded.

According to the experimental groups, the trans-well systems were filled with 100 µL of maturation medium or 233 µL: aMEM, 20% FBS, 1% glutamine (Cat. No. BE17-605E/U1 Lonza), antibiotics such as 75 mg/L of penicillin-G and 50 mg/L of streptomycin sulfate (Cat. No. DE17-602E Lonza). The hormonal trigger for oocyte maturation was established to be 25 IU/mL of human Chorionic Gonadotropin (hCG: equivalent to 6 µg/mL Chorulon®, MSD Animal Health S.r.l., Segrate, Italy), as previously validated [58]. The hCG's biological activity was declared to be 5000 IU per vial in accordance with the manufacturer's instructions.

EA follicles were left in an incubator at 38.5 °C and 5% CO_2, and the oocyte maturation performances were assessed after 24 h of IVM.

Meiotic and developmental competences of low competent oocytes derived from EA

Oocyte nuclear stage assessment

The in vitro matured oocytes under FEO protocols were denuded of surrounding cumulus cells, permeabilized/fixed in a solution of acetic acid and ethanol (1:3) for at least 12 h, and finally stained with 1% Lacmoid (Cat. No. 274,720, Sigma) solubilized in distilled water. Then, the oocytes were mounted on the object slide and analyzed under a Phase Contrast Microscope (AxioVert, Carl Zeiss, Jena, Germany) for the detection of the nuclear stage.

The oocytes were classified according to the meiotic nuclear stages in Germinal Vesicle (GV), Germinal Vesicle Break Down (GVBD)/Metaphase I (MI), and Metaphase II (MII) according to [68].

Laser confocal microscopy analysis for oocyte chromatin configuration assessment

The oocytes in the GV stage, not subjected to a maturation protocol, were immunoassayed with Propidium Iodide (PI; 1 mg/ml) staining solution (Cat. No. P4864, Sigma) to evaluate their chromatin configuration.

Observations of the red fluorescence probe were performed with a Bio-Rad laser scanning confocal microscope (Radiance 2000 IK-2, Hemel Hempstead, UK) equipped with a krypton/argon ion laser. The samples were analyzed with an inverted microscope (Zeiss Axiovert, Oberkochen, Germany) equipped with a plan-apochromat oil immersion objective 636 magnification/1.4 numerical aperture (NA). Immunoassayed oocytes were observed using the visible lines of excitation of 488 nm and a dichroic filter (560LP, Bio-Rad). Digital optical sections were obtained by scanning the sample on the z-axis at 0.2 mm of thickness throughout the plane of focus containing the GV equatorial plane (620 mm). For each experiment, all the categories of oocytes were compared, maintaining similar gain and laser parameters.

The oocyte chromatin configuration was evaluated according to [68]. In brief, the z-series obtained were merged to produce a two-dimensional image showing the staining pattern and the Total Fluorescence Intensity (TFI) emitted by each GV. The TFI emitted from each GV was measured using the LaserPix software (Bio-Rad).

Parthenogenetic activation

To determine the degree of cytoplasmic maturation, parthenotes were produced by activating MII oocytes identified for the extrusion of the first polar body under the stereomicroscope. The parthenogenetic competence assessment was performed on MII oocytes derived from the FEO maturation protocol and compared with that of MII oocytes isolated from medium antral follicles (positive Ctr). Parthenogenetic activation was carried out according to a previously validated protocol [68]. After 72 h from activation, both uncleaved and cleaved oocytes were analyzed under an inverted microscope (time-lapse imaging software NIS-Elements (Eclipse Ti Series, Nikon, Japan) to evaluate their developmental stage by counting the number of blastomeres. The presence of nuclei was confirmed using Lacmoid staining (Sect. Oocyte nuclear stage assessment) through phase contrast microscopy.

Biochemical analyses

Real-time qPCR

The total RNA was extracted with a Single-Cell RNA Purification Kit (Norgen Biotek Corp. Cat 51,800) following the manufacturer's instructions. A total of 1 µg of total RNA was retrotranscribed using oligodT primers (Bioline, London, UK) and Tetro Reverse Transcriptase (Bioline, London, UK), following the manufacturer's instructions. The qPCRs were carried out in triplicate using the SensiFAST SYBR Lo-ROX kit (Bioline London, UK) on a 7500 Fast Real-Time PCR System (Life Technologies, Carlsbad, CA, USA), according to the manufacturer's instructions. The following PCR conditions were used for all the experiments: 95 °C for 10 min, followed by 40 cycles at 95 °C for 10 s and 60 °C for 30 s. Relative quantification was performed by using the ΔΔCt method. GAPDH (Glyceraldehyde 3-phosphate dehydrogenase) and YWHAZ (Tyrosine 3-Monooxygenase/Tryptophan 5-Monooxygenase Activation Protein Zeta) were selected amongst the housekeeping genes for gene quantification. The expression profiles were similar with both reference genes. Three independent biological replicates were performed. For each *iv*F group (AO_{5PA} and Ctrl), 30 EA-follicular walls were collected and processed for gene expression at the end of in vitro culture, respectively. The primer sequences are reported in Table 1.

Statistical analysis

Three independent experimental replicates were performed. The data are presented as the percentage or mean ± SD. GraphPad Prism 9 (GraphPad Software) was used for the statistical analyses, and values with $p<0.05$ were considered statistically significant.

Differences in antrum formation, oocyte meiotic competence acquisition and parthenogenetic development in vitro between different groups were evaluated by multiple unpaired t-test using the Holm-Šídák method and by ordinary one-way ANOVA followed by the Dunnett test to compare multiple groups. All the other data were analyzed by an unpaired t-test.

Results

*iv*F outcomes demonstrated that patterned electrospun-PCL scaffold support multiple follicle development

To verify the possibility of patterned electrospun PCL scaffolds to support multiple PA follicle development, an

Table 1 Sequences of primers used in real-time qPCR

Gene	Forward Sequence	Reverse Sequence
CYP11A1	5′-CTCGATCCTTCAATGAGATC-3′	5′-TACAACACTGGTGATGGACT-3′
CYP17A1	5′-ACTCTAGGCCTCTTGTCGGACCAA-3′	5′-CAACCACGGGAATATGTCCACCAG-3′
CYP19A1	5′-TCGTCCTGGTCAACCCTTCTG-3′	5′-CCAGACGAGACCAGAGACCG-3′
GAPDH	5′-TCGGAGTGAACGGATTTGGC-3′	5′-CCGTTCTCTGCCTTGACTGT-3′
YWHAZ	5′-AGACGGAAGGTGCTGAGAAA-3′	5′-CGTTGGGGATCAAGAACTTT-3′

engineered ovary enriched in 5 PA follicles (AO_{5PA}) was used and compared with the validated single follicle PCL-based *iv*F protocol (Ctrl).

Both AO_{5PA} and Ctrl protocol supported follicle development by inducing a very low percentage of follicle degeneration (for both <9%; $p=0.3280$). On the contrary, the majority (>91%) of 221 PA follicles after 14 days of culture were transited towards the EA stage independently of the *iv*F protocol adopted (Ctrl *vs.* AO_{5PA}; $p=0.3346$), as summarized in Fig. 2.

However, in vitro follicle development under AO_{5PA} culture condition was slowed. Indeed, only 46.6% of PA follicles differentiated the antrum cavity after 12 days of incubation instead of 85% under Ctrl ($p<0.0003$; Fig. 3A). In addition, the final diameter of EA follicles obtained using AO_{5PA} was significantly smaller than that of the Ctrl group (367.3±11; Δ growth: 49.6% *vs.* 416.7±11; Δ growth: 65.6% ($p<0.0001$) respectively; Fig. 3B).

Single and multiple follicles-PCL based *iv*F induced a steroidogenic activation in EA follicles

CYP11A1, *CYP17A1*, and *CYP19A1* expression were evaluated on EA follicle walls at the end of incubation (14 days) under Ctrl and AO_{5PA} protocol (Fig. 4) and compared with in vivo EA structures.

Under in vivo folliculogenesis, the transition from PA to EA is accompanied by an upregulation of *CYP17A1* and *CYP19A1* (PA *vs.* EA, 1.4-fold and 2-fold upregulation, respectively), while the expression of *CYP11A1* does not undergo any changes (Fig. 4).

Analogously, *CYP19A1* (approximately 2-fold) and *CYP17A1* (for both approximately 1.6-fold) were upregulated in EA follicles obtained from both *iv*F protocols but, on the contrary, also a significant overexpression of *CYP11A1* was observed (AO_{5PA} and Ctrl *vs.* in vivo EA; $p<0.0001$).

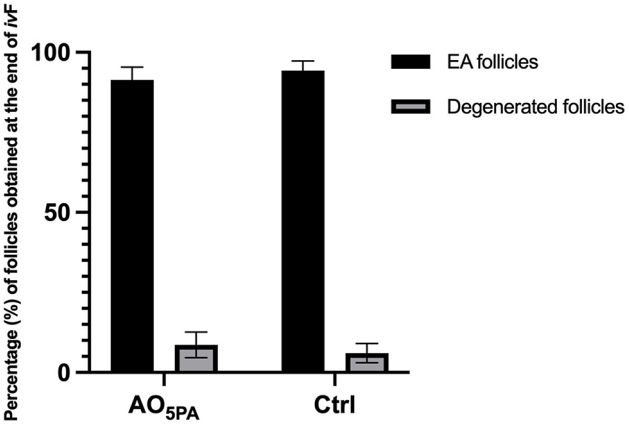

Fig. 2 Percentage (%) of EA and degenerated follicles obtained after 14 days of *iv*F carried out under single and multiple follicles (AO_{5PA}) set up. Three independent biological replicates were performed. A total of 115 and 106 follicles were cultured under artificial ovary (5 PA on PCL scaffold: AO_{5PA}) or Ctrl (single PA scaffold-mediated culture), respectively

Oocytes grown under both PCL-based single and multiple *iv*F achieved the full dimension and improved their meiotic competence

As summarized in Table 2, the majority of cumulus oocyte complexes (COCs) isolated from EA follicles obtained under both AO_{5PA} and Ctrl protocols were classified as healthy (>90%; $p=0.7892$). In addition, all the enclosed oocytes reached the fully grown dimension (oocyte diameter of both in vitro EA *vs.* in vivo EA; $p=0.8542$).

Most of the oocytes developed in vitro acquired the functional ability to resume the meiotic cell cycle in response to hCG stimulation (25 IU/mL), even if their percentage resulted significantly lower than that recorded in in vivo EA (Fig. 5).

Indeed, during the transition from PA to EA, most of the oocytes enclosed into in vivo EA resume meiosis under FEO (GVBD/MI+MII: 87.8%; PA *vs.* EA; $p<0.0001$) *vs.* approximately 80% of oocytes enclosed in *in vitro* EA (76.4% and 82.8% for AO_{5PA} or Ctr, respectively; $p>0.2917$). Of note, only half of the oocytes grown in vitro reached the MII stage (45.5% *vs.* 45.4%, respectively; $p>0.9996$) instead of 71% of in *vivo*-EA-derived ones (for both: $p=0.005$).

Therefore, PCL-patterned scaffold was highly biomimetic to substitute the ovarian matrix during the transition from multiple PA to EA stage by ensuring, at the same time, an adequate environment to support oocyte development at morphological (fully grown dimension) and functional (>80% acquired the meiotic competence) level.

Strengthening multiple follicle-based *iv*F did not compromise the ability of PCL-patterned scaffold to guide PA follicle growth and oocyte development

Once the AO_{5PA} protocol was tested, a second step was performed to investigate whether the *iv*F culture could be implemented by increasing the number of PA follicles on scaffold basis. In order to compare the biological outcomes, the ratio between scaffold surface/culture media volume has been maintained during both AO cultures. To this aims, 10 PA (AO_{10PA}) were cultured on 0.7 cm^2 of PCL support using 48 multi wells/ 233 µL media instead of 5 PA (AO_{5PA}) on 0.3 cm^2 of scaffold in 96 multi wells/100 µL media.

The implemented AO *iv*F protocol (AO_{10PA}) was totally compatible with follicle survival (degenerated follicles: < 5%) and development (Fig. 6A and B).

Indeed, most of the AO_{10PA}*iv*F-derived follicles reached the EA stage (100 out of 130 incubated PA), although in a smaller percentage (*vs.* AO_{5PA} and Ctrl; $p=0.0016$).

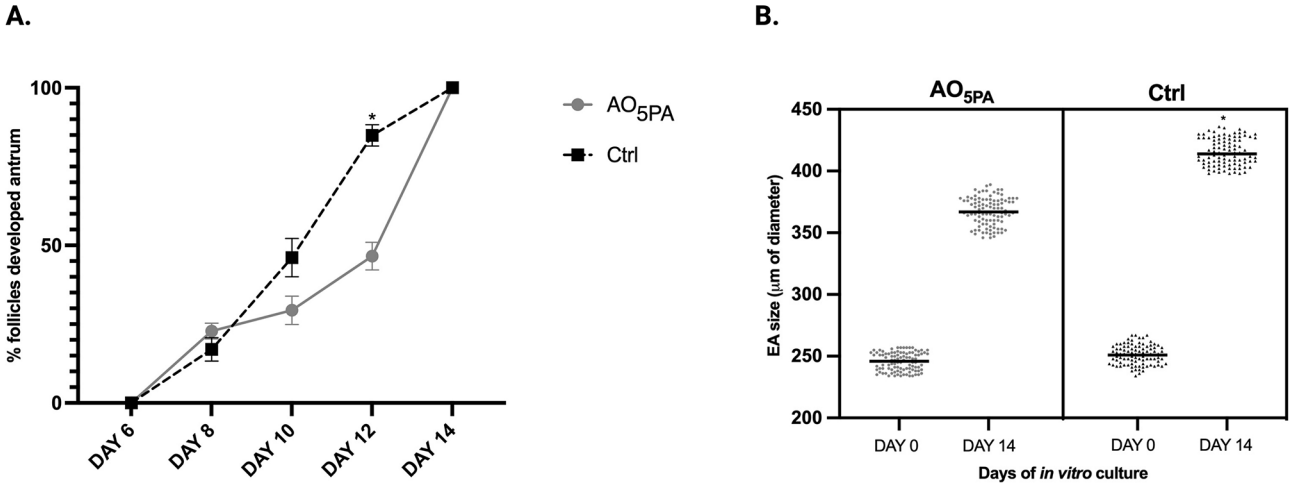

Fig. 3 (**A**) Kinetic of antrum development during *iv*F carried out under Ctrl and AO_{5PA} conditions. Three independent biological replicates were performed starting from 115 and 106 PA follicles for AO_{5PA} and Ctrl, respectively. The differentiation of the antrum cavities during *iv*F cultures was recorded under the stereomicroscope. Superscripts indicated statistically significant values (*; $p < 0.05$). (**B**) PA in vitrogrowth carried out on PCL scaffold using multiple (AO_{5PA}) and single follicle *iv*F (Ctrl). Three independent biological replicates were performed starting from 115 and 106 PA follicles for AO_{5PA} and Ctrl, respectively. After 14 days of culture, follicle size was determined exclusively in follicles that had developed antrum cavity (105 and 100 EA follicles, respectively). Superscripts indicated statistically significant values (*; $p < 0.05$)

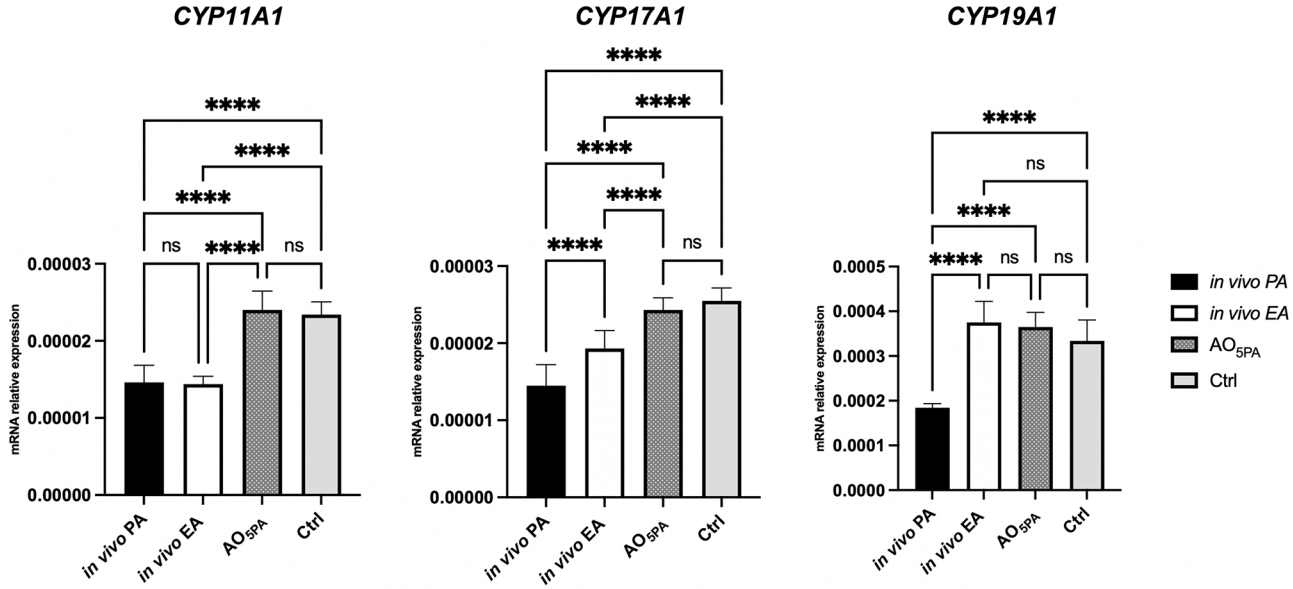

Fig. 4 Expression profiles of the main steroidogenic enzymes analyzed on EA follicle walls obtained using Ctrl and AO_{5PA}protocol. Three independent biological replicates were performed. For each *iv*F group (AO_{5PA} and Ctrl), 30 EA-follicular walls were collected and processed for gene expression at the end of in vitro culture, respectively. Superscripts indicated statistically significant values (****; $p < 0.0001$)

Surprisingly, approximately 17% of these follicles, after 14 days of incubation, appeared to be healthy but still at the PA stage (Fig. 6A).

A clear delay in antrum cavity differentiation was recorded under AO_{10PA} on Day 12 (in AO_{5PA} and AO_{10PA} - 44% of EA follicles *vs.* 84% in Ctrl; $p < 0.0007$). The result became even more evident on Day 14 when only 80% of them displayed the antrum cavity instead of 100% in both Ctrl and AO_{5PA} protocols (Fig. 6A).

In addition, follicles growth (25.2% less than Ctrl; $p < 0.0001$; Fig. 6B) was also lower in AO_{10PA} and in AO_{5PA} (22% less than Ctrl; $p < 0.0001$).

PCL-patterned matrix drove oogenesis even under the implemented multiple follicle-based *iv*F

Approximately 90% of EA developed using the AO condition released healthy COCs enclosing a fully grown oocyte, independently of the *iv*F protocol used (Table 3).

Table 2 Gamete morphological indexes before and after *iv*F carried out under PCL-based single and multiple *iv*F

ivF groups	Healthy COCs (COCs/EA follicles)	Oocyte starting diameters	Oocyte final diameters
	(%)	(μm ± SD)	(μm ± SD)
in vivo PA	84	75±6	-
in vivo EA	90	-	114±8
AO_{5PA}	90.6	76±5	116±4
Ctrl	91.3	77±6	111±5

Three independent biological replicates were performed using exclusively EA follicles obtained at the end of *iv*F cultures. Not statistically significant values were recorded

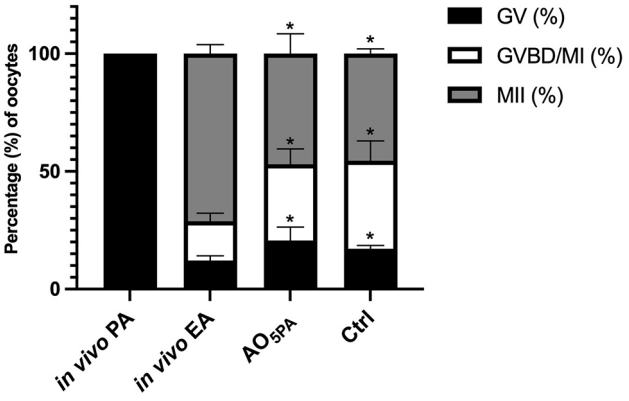

Fig. 5 Resumption of meiosis in *in vivo vs. in vitro* grown oocytes. Three independent biological replicates of FEO maturation were performed to compare the in vivo PA and EA follicles with the EA ones developed under both single and multiple *iv*F protocols. Superscripts indicated statistically significant values (* *vs.* in vivo EA; $p < 0.05$). Of particular importance, oocytes derived from PA are consistently found in the GV stage, a statistically significant finding when compared to all other groups ($p < 0.0001$). GV: Germinal Vesicle; GVBD, Germinal Vesicle Break Down; MI, Metaphase 1; MII, Metaphase 2

Of note, the highest meiotic competence was expressed from oocytes grown under the AO_{10PA}*iv*F protocol, thus confirming the biomimicry of PCL to support multiple oocytes in vitro development (GVBD/MI+MII: 100% *vs.* 81%; $p=0.0002$ and 82.5%; $p=0.0003$ of AO_{5PA} and Ctrl, respectively; Fig. 7). Moreover, the AO_{10PA} protocol also turned out to be the culture context where oocytes achieved an improved meiotic competence (62% *vs.* 46% and 45% of AO_{5PA} and Ctrl, respectively; for both $p=0.02$).

Based on the achieved results, the AO_{10PA} protocol was successfully tested in *iv*F, thus building up a proof of concept of PCL biomimicry in bringing the simultaneous transition of 10 PA towards the EA stage without compromising the viability and functionality of both somatic and germinal compartment.

PCL-based multiple *iv*F is ideal for setting up long-term PA follicle incubation

Based on the previous results, 18 days *iv*F was tempted in order to verify whether PCL-patterned scaffold can support long-term AO_{10PA} protocol by maximizing multiple recruitment of PA towards EA.

Long-term *iv*F did not determine any improvement in follicle growth (366±13 μm 18 days *vs.* 350±8 μm 14 days; $p>0.05$), but positively impacted follicle survival and development (Fig. 8A and B). Indeed, long-term AO_{10PA} significantly increased the number of recruited EA follicles (92% at day 18 *vs.* 74.7% at day 14; $p<0.001$) without affecting follicle survival (16 degenerated out of 200 PA). On the contrary, prolonged incubation had adverse effects on Ctrl *iv*F, with a significantly higher occurrence of degenerated follicles (120 out of 230 PA incubated) and a decrease in EA follicle recruitment (48% *vs.* 90% after 14 days, respectively; $p<0.001$) observed (see Fig. 8). Additionally, a lower expression of the steroidogenesis-related gene *CYP19A1* was noted compared to the AO10PA Group (1.3-fold change increase vs. Ctrl; $p=0.008$; Fig. 8C).

Long-term PCL-based *iv*F guided multiple oocyte development favoring large chromatin remodeling and meiotic competence achievement

Long-term AO_{10PA} protocol did not influence oocyte growth ($p>0.05$; 18 days *vs.* 14 days), but the oogenesis process (Figs. 9 and 10, and Fig. 11).

Interestingly, long-term AO_{10PA} protocol was essential to promote a more advanced large chromatin remodeling (Fig. 9A): in fact, long-term *iv*F switched on the process of chromatin rearrangement if carried out under multiple protocols. Specifically, long-term AO_{10PA} enabled 73% of in vitro grown oocytes to arrange chromatic reaching the mature SN and SNE configurations. More in detail, half of these oocytes left the immature NSN chromatin configuration to move towards the SN one, like the oocyte belonging to in vivo EA follicles (50% *vs.* 62%; $p>0.05$). Of note, 23% of them acquired the final SNE pattern, thus suggesting that long-term PCL-based culture supported a germinal compartment advancement (23% *vs.* 0% in vivo EA). Indeed, the process of large chromatin remodeling moved towards the final outcome of oocytes recorded exclusively in oocytes enclosed in small antral (SA) follicles (52%, see Fig. 9).

The enhanced development of the oocytes grown under long-term AO_{10PA} was further supported by the analysis of their nuclear stage after FEO maturation (Fig. 10).

Indeed, approximately 90% of them were able to resume meiosis in response to hCG stimulation (GVBD/MI+MII 92.5% *vs.* 87.8% in vivo EA; $p>0.05$) and more than half reached the MII stage (MII 67% *vs.* 71.1% in vivo EA; $p>0.05$; Fig. 10). Notably, single follicle

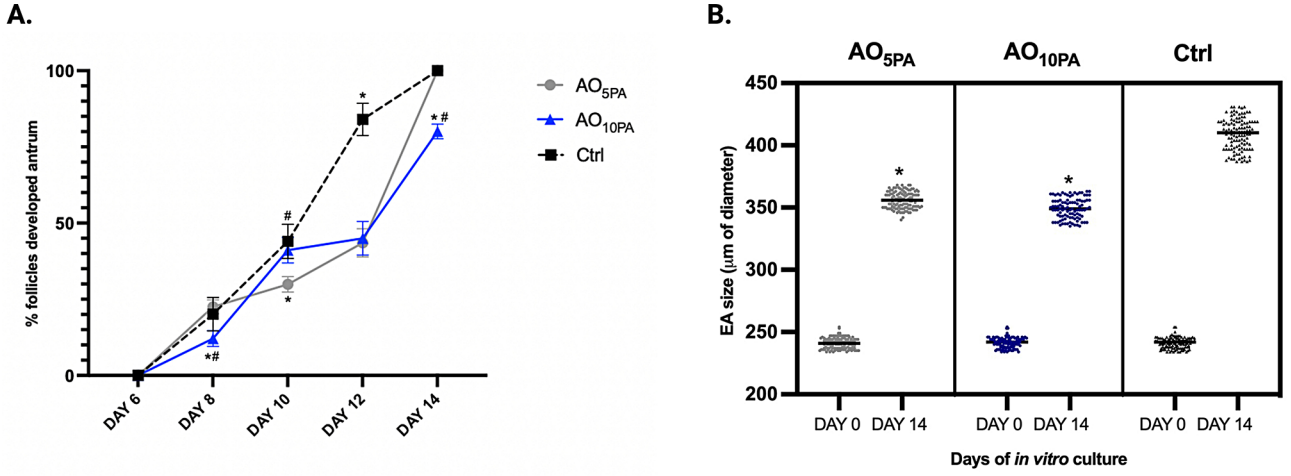

Fig. 6 (**A**) Kinetic of antrum development during*iv*F carried out under Ctrl and multiple ***iv***F protocols (AO_{5PA} and AO_{10PA}). Three independent biological replicates were performed, starting from 130 follicles per group. The differentiation of the antrum cavities during *iv*F cultures was recorded under the stereomicroscope in morphologically healthy follicles. Superscripts indicated statistically significant values: **vs.* Ctrl group ($p < 0.05$); $^{\#}$*vs.*AO_{5PA} well ($p < 0.05$). (**B**) PA in vitro growth carried out on PCL scaffold using two multiple (AO_{5PA}vs. AO_{10PA}) and single follicle protocols (Ctrl) in comparison. Three independent biological replicates were performed. A total of 120, 100 and 117 EA follicles are obtained from 130 PA used in each AO_{5PA}, AO_{10PA} and Ctrl *iv*F condition, respectively. Superscripts indicated statistically significant values: **vs.*EA follicles (Ctrl; Day 14) for $p < 0.05$

Table 3 Comparison of gamete morphological indexes amongst PCL-based*ivF* protocols

ivF groups	Healthy COCs (COCs/EA follicles)	Oocyte starting diameters	Oocyte final diameters
	(%)	(µm ± SD)	(µm ± SD)
AO_{5PA}	93	77± 4	112±5
AO_{10PA}	94	78± 5	113±3
Ctrl	89	79±5	115±7

Three independent biological replicates were performed using EA follicles exclusively at the end of *iv*F cultures. Not statistically significant values are analyzed

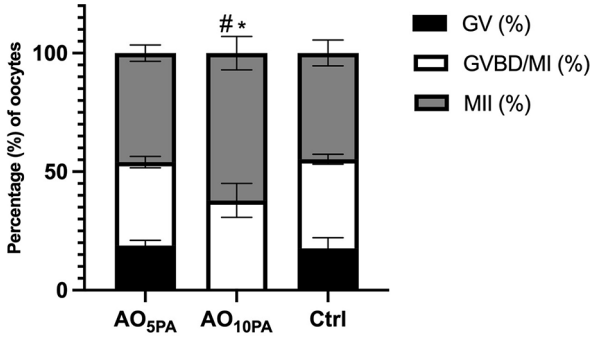

Fig. 7 Comparison of hCG-induced meiotic resumption in EA follicle obtained using PCL-based *iv*F multiple protocols. Three independent biological replicates of FEO maturation techniques were performed to compare the meiotic competencies of oocytes isolated from in vivo PA and EA follicles *vs.* those of oocytes derived from *iv*F EA follicles developed under Ctrl and both AO *iv*F protocols (AO_{5PA}*vs.*AO_{10PA}). Different nuclear stages were recorded: Germinal Vesicle stage, GV: GVBD, Germinal Vesicle Break Down; MI, Metaphase 1; MII, Metaphase 2. Superscripts indicated statistically significant values: **vs.*AO_{5PA}; $^{\#}$ AO_{10PA}*vs.*Ctrl; $p < 0.05$

long-term *iv*F (Ctrl), although negatively impacted the percentage of healthy available COCs (48% 18 days *vs.* 92% 14 days; $p<0{,}001$), did not affect the acquisition of the meiotic competence (GVBD/MI+MII: 82.5% *vs.* 81%, respectively for Ctrl group cultured for 14 days or 18 days; $p>0.05$).

Finally, the degree of cytoplasmic maturation expressed by the in vitro-grown oocytes was tested by performing a comparative study to exploit the parthenogenetic activation assay (Fig. 11).

As summarized in Fig. 11A, embryo development recorded after 3 days from parthenogenetic activation in long-term AO_{10PA}-derived oocytes was superimposable to that of SA-enclosed ones (81.4% activated oocytes *vs.* 85%; $p>0.05$). On the contrary, most oocytes grown under Ctrl protocol were unaffected by parthenogenetic activation by remaining uncleaved (74.8% *vs.* 18.2% and 15% of AO_{10PA} and SA, respectively; for both $p<0.0001$).

The engineered ovarian model adopted for our in vitro screening proves that patterned PCL scaffolds can be considered to develop innovative REPROTEN strategies for biomedical applications addressed to treat female infertility as well as for providing great potential to advance *iv*F culture systems.

Indeed, the present results altogether confirm the total adequacy of patterned electrospun fibrous PCL scaffold in replacing the ovarian matrix during follicle transition from preantral to antral stage. The ovarian bioinspired PCL scaffold also has the merit of maintaining its biocompatibility over the long term, thus guiding the germinal compartment towards the stepwise process of

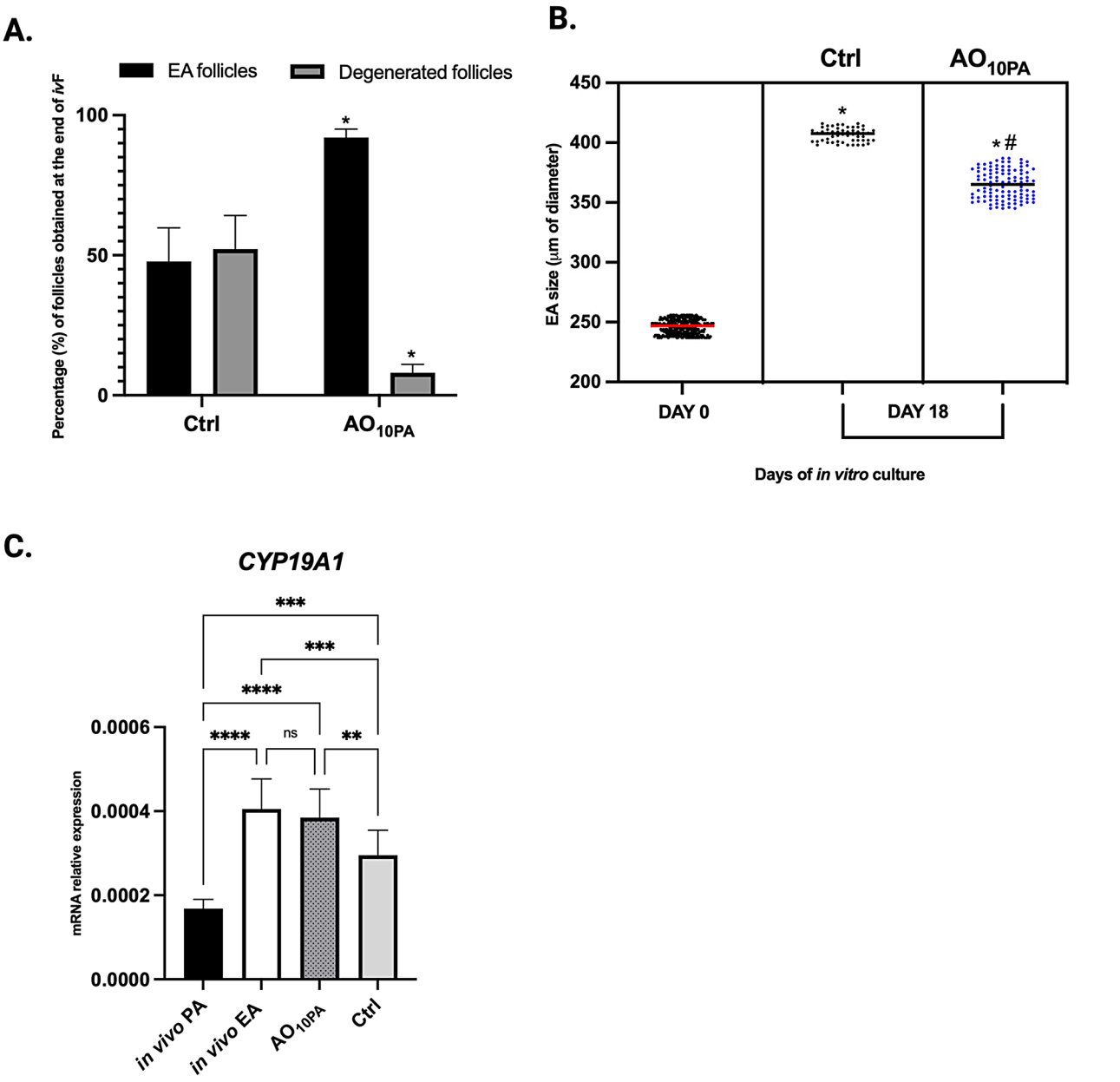

Fig. 8 Somatic compartment performance of PA follicles grown under long-term *iv*F (18 days) carried out using single and multiple follicles (AO_{10PA}) protocols. (**A**) Incidence of EA and degenerated follicles in long-term *iv*F. Three independent biological replicates were performed. 184 and 110 out of 200 and 230 cultured PA follicles reached the EA stage, whereas 16 and 120 of them degenerated under AO_{10PA} and Ctrl *iv*F, respectively. Superscripts indicated statistically significant values: **vs.*Ctr; $p < 0.05$. (**B**) Comparison of PA in vitrolong-term growth carried out on multiple (AO_{10PA}) and single PCL-based *iv*F protocols (Ctrl). Three independent biological replicates were performed. A total of 200 and 230 PA follicles per group were cultured for 18 days, adopting AO_{10PA} and Ctrl protocols. Superscripts indicated statistically significant values: **vs.*Day 0; $^{\#}$*vs.*Ctr 18 days of *iv*F; $p < 0.05$. (**C**) CYP19A1 expression pattern in EA follicles developed in long-term *iv*F. Three independent biological replicates were performed using 60 follicular walls of in vitro EA follicles obtained under AO_{10PA} and 50 follicular walls under Ctrl, respectively, and 50 follicle walls isolated from in vivo EA. The corresponding oocytes were used for the analysis of chromatin remodeling. Superscripts indicated statistically significant values; $p < 0.05$)

A.

Follicle stage	Follicle source	Oocytes analyzed	Chromatin configuration in GV oocytes		
		(*n*)	NSN	SN	SNE
			(%±SD)	(%±SD)	(%±SD)
EA	*in vivo*	80	37.8±9	62.2±9	*nd*
SA		82	*nd*	47.6±2	52.4±2
CTRL	*14 days ivF*	70	61.7±3*	38.3±3*	*nd*
AO_{10PA}		65	59.3±10*	40.7±10*	*nd*
CTRL	*18 days ivF*	50	100±0*#$	*nd*	*nd*
AO_{10PA}		60	26.7±8	50±5	23.3±8#

B.

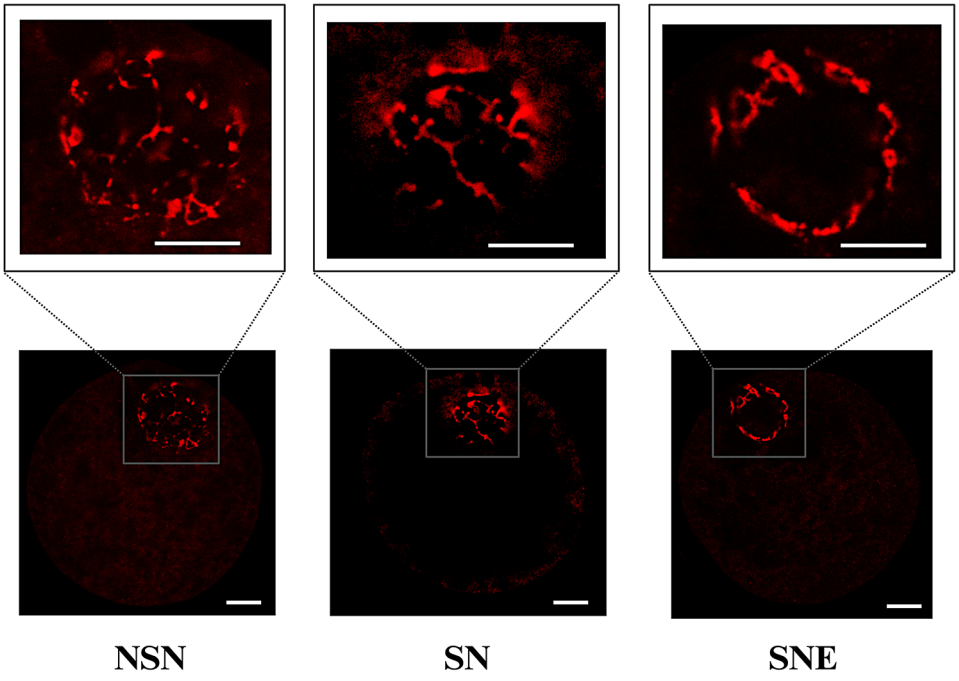

Fig. 9 Chromatin configurations in GV oocytes isolated from follicles developed in vivo (EA and SA) or in vitro (Ctrl and AO_{10PA}). (**A**) Comparison of the three major chromatin configuration patterns in antral-enclosed oocytes recruited in vivo or in vitro using PCL-based *iv*F protocols. Three independent biological replicates were performed. Superscripts indicated statistically significant values: *vs.* in vivo EA; #*vs.* in vivo SA; $vs.$AO_{10PA}$ (18 days *iv*F); $p < 0.05$. (**B**) Example of chromatin configuration analyzed in GV in vitro grown oocytes. Confocal images of sheep GVs showing the three major chromatin configurations: NSN, Non-Surrounding Nucleolus; SN, Surrounding Nucleolus and SNE, Surrounding Nuclear Envelope/SNE. DNA staining was performed using Propidium Iodide (red fluorescence). *Upper panel*: 10 µm; *Lower panel*: scale bar: 30 µm

specialization leading to meiotic and developmental competence acquisition.

Discussion

The development of an artificial ovary stands as a pivotal facet within the field of REPROTEN, its successful realization contingent upon the faithful recapitulation of ovarian folliculogenesis [17, 18, 69]. This intricate process entails the utilization of immature follicles and their guidance through advanced stages until the attainment of fully-grown oocytes to be enrolled in vivo towards follicle dominance or in ART towards IVM-IVF protocols [28, 30]. These biomedical innovations may profoundly impact open female reproductive issues, such as fertility preservation in young oncological patients [25, 70]. Despite the successful cryopreservation outcomes of ovarian tissue and concurrent scientific evidence of successful transplantation leading to the restoration

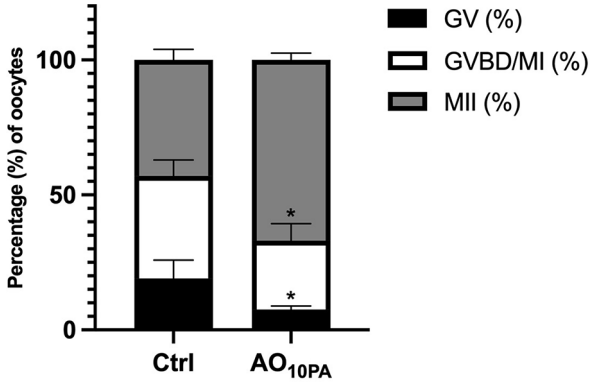

Fig. 10 Comparison of meiotic competence of in vitro grown oocytes obtained under long-term PCL-based *iv*F carried out using single and multiple (AO_{10PA}) protocols. Three independent biological replicates were performed on a total of 111 and 57 EA follicles obtained under AO_{10PA} and Ctrl *iv*F protocols, respectively. Superscripts indicated statistically significant values: **vs.*Ctrl for $p < 0.005$. GV: Germinal Vesicle; GV: Germinal Vesicle Break Down; MI: Metaphase I; MII: Metaphase II

of cyclicality, the risk of transplanting cancerous cells necessitates the exploration of alternative strategies. The development of engineered ovaries could offer a viable solution by utilizing biomaterials tested not only for biocompatibility but also for mimicking the ovarian matrix in various stages of folliculogenesis. More in detail, engineering immature follicles derived from cryopreserved ovarian tissue of cancer patients on a bioinspired ovarian scaffold may represent a valid and safe alternative since it strategically mitigates the risks associated with inadvertent malignant cell transfer [20, 28, 30, 71]. In light of this, the development of a bioengineered artificial ovary aims to replicate the intricate native ovarian system, necessitating a biocompatible scaffold for encapsulating isolated follicles and/or autologous ovarian cells [29, 72]. In this context, biomimetic scaffolds can be used to optimize current *iv*F protocols by leveraging an ovarian mimetic approach, potentially mimicking the gonadotropin-insensitive or low-sensitive phases of folliculogenesis [72, 73]. Among these, PCL electrospun fibrous scaffold produced by "green-electrospinning" technology has ventured into engineered reproductive materials, representing a novel focus in the field, albeit currently explored by only a few research groups [51, 52, 54]. Recent results with PCL have shown promise, offering not only clinical usability but also long-term biocompatibility [74–78]. Our previous study further demonstrates that PCL serves as a supportive scaffold, enabling individual follicles to undergo the gonadotropin-sensitive phase of folliculogenesis and transition from the preantral to the early antral stage [56]. This establishes the foundation for subsequent in vivo selection by gonadotropins during the early antral phase, underscoring its potential to mimic natural follicular development effectively. While PCL holds promise, demonstrating its capability to sustain the simultaneous survival and growth of multiple follicles remains a formidable challenge. This represents a critical milestone in affirming its suitability for constructing an artificial ovary that faithfully emulates the complexities of the natural follicular environment.

Within this framework, the current study aims to juxtapose a validated single-follicle in vitro culture method (Ctrl) [56] with the novel multiple follicle-on-scaffold procedure within the REPROTEN context (AO) to functional validate the biocompatibility of patterned-electrospun fibrous scaffolds fabricated with PCL, an FDA approved biomaterial [79, 80]. To mimic the behavior of PA-engineered PCL after in vivo transplantation, the sequential step-wise phases of follicle growth and oocyte maturation have been simulated in vitro and assessed on both the somatic and germinal compartments.

Based on our findings, PCL in vitro can be successfully adopted to support multiple PA follicle growth by reproducing a long-term favorable microenvironment to guide an advanced follicle and oocyte in vitro development.

The 3D culture employing an engineered-PCL scaffold with multiple PA constructs has demonstrated compatibility with the long-term survival of ovarian structures, exhibiting significant growth (Δ growth: 48%) and consistently promoting antral differentiation in the majority of incubated follicles. Particularly noteworthy is the observed positive paracrine cross-talk among follicles within the multiple-system during culture, a phenomenon absents in the single-system setup. Notably, follicles exhibit a decelerated growth rate, prolonged viability, and heightened steroidogenic activity. This mechanism closely mirrors the physiological processes observed in vivo, wherein the cohort of antral follicles transitions from gonadotropin sensitivity to dependence [81].

This data underscores the sustained follicular performance observed during *in vitro* culture, emphasizing the intricate regulation of steroid hormone production throughout follicle growth and its pivotal role in supporting the development of fully competent oocytes and subsequent reproductive processes. In particular, aromatase activation in ovarian folliculogenesis is of critical importance due to its involvement in orchestrating the hormonal dynamics essential for optimal follicular progression [82–84]. This regulatory process not only impacts oocyte quality but also significantly influences the overall success of reproductive outcomes. Thus, understanding and manipulating steroid hormone regulation are crucial steps in enhancing the journey from follicular development to successful reproduction [12, 85, 86].

The positive effect of the long-term AO_{10PA} system on oocyte development further corroborates the PCL's capacity to accurately mimic the ovarian microenvironment. By facilitating a gradual follicular growth rate,

A.

Follicle stage	Follicle source	Oocytes Analyzed	Embryo stage after 72h from activation			
		(*n*)	Uncleaved (%±SD)	Activated (PN) (%±SD)	< 8 nuclei (%±SD)	> 8 nuclei (%±SD)
SA	*in vivo*	120	15±2.5	25±2.5	29.2±5	30.8±5
Ctrl	18 days *iv*F	66	74.8±6*	28.2±9	-	-
AO_{10PA}		64	18.2±4.5#	25.8±5	22.7±4.5*#	33.3±7#

B.

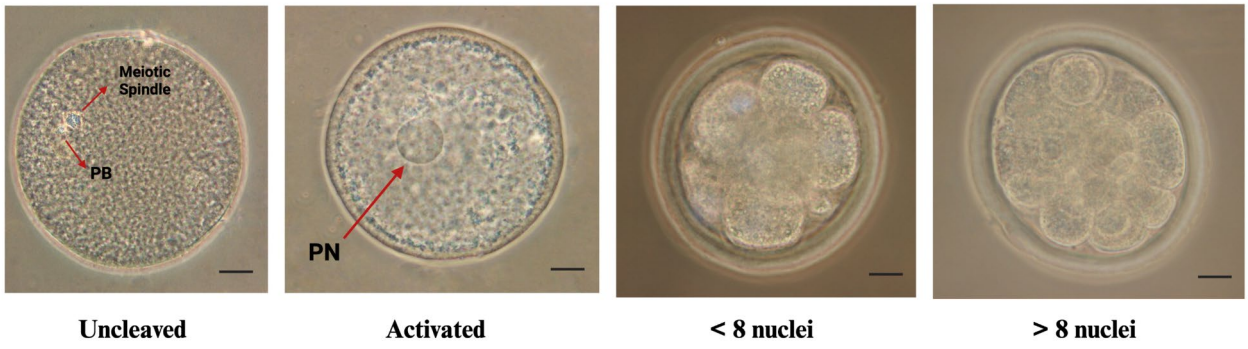

Fig. 11 Parthenogenetic activation of in vitro grown oocytes obtained under PCL-single and multiple *iv*F. (**A**) Embryo development recorded after 72 h from parthenogenetic activation. The parthenogenetic activation was performed on MII oocytes obtained from EA developed in vitro or from small antral (SA) follicles grown in vivo (positive Ctr). Three independent biological replicates were performed. Superscripts indicated statistically significant values: *vs. in vivo SA; #vs. Ctrl; $p < 0.05$. (**B**) Representative images of key moments of embryo development after 3 days from parthenogenetic activation. The illustrative figures represent the major stages of parthenogenetic development recorded in sheep oocytes grown *in vitro* using single (Ctrl) or multiple (AO_{10PA}) *iv*F protocols: uncleaved oocyte, pronuclear (PN) stage, embryo development at < 8-nuclei and > 8-nuclei. The oocytes/embryos are stained with Lacmoid, and the images are captured using bright field microscopy at 40× magnification: scale bar: 30 µm

the PCL scaffold creates an environment conducive to the effective differentiation process of enclosed oocytes. This phenomenon aligns with the physiological scenario within the ovary, where controlled follicular growth is essential for optimal oocyte maturation. Thus, the ability of the PCL scaffold to replicate such dynamics highlights its potential to provide a more physiologically relevant platform for in vitro follicle development studies and underscores its significance in advancing reproductive research and technology. Indeed, long-term *iv*F on PCL fibers promoted a significant advancement in oocyte differentiation by supporting advancement in the process of large chromatin remodeling. Here, the critically analyzed results reveal that PCL effectively supports oocyte development, culminating in the transition from the NSN to SN configuration over the long term. This transition represents a significant functional milestone during sheep oogenesis, physiologically achieved by approximately 60% of oocytes enclosed within EA follicles. However, follicular antrum differentiation in vitro does not always coincide with this oocyte functional target. Indeed, oocyte engagement in chromatin remodeling occurs only when follicular development is delayed, as seen in the single follicle oil system [68, 87] or in the current 3D AO_{10PA} long-term system. Nevertheless, a comparison between the two systems reveals that, for the first time, a culture system has successfully promoted the acquisition of the final configuration in a substantial proportion of oocytes (20%), resembling the SNE configuration observed in sheep [87]. Consistently, the chromatin configuration is highly species-specific, as demonstrated by Russo et al., where in sheep, the mature configuration observed in oocytes enclosed within preovulatory follicles is consistently SNE in 100% of cases [87]. This finding affirms the compatibility of the culture system developed utilizing PCL as an ovarian matrix with efficient germinal compartment development. Initiation of oocytes within the 3D AO_{10PA} system results in an advanced stage of chromatin remodeling after 18 days of *iv*F, surpassing the stage recorded in oocytes isolated from physiologically grown EA follicles and intermediate to that observed in oocytes residing within SA follicles (52% SNE).

Chromatin remodeling plays a crucial role in extending current in vitro protocols to an in vivo setting, facilitating the acquisition of evolutionary competence in oocytes derived from immature developmental-stage follicles [88–90]. This process is essential to support the correct progression of meiotic resumption and subsequent oocyte activation [91]. Additionally, chromatin remodeling has been linked to oocyte developmental competence, as evidenced by the development of pre-in vitro maturation protocols. These protocols utilize a culture medium containing cumulus-oocyte complex ligand-receptor signaling molecules to maintain meiotic arrest, aiming to promote synergistic chromatin development [92–95]. Expanding on this concept, the higher degree of competence observed in oocytes at a more advanced stage of chromatin configuration appears to be indirectly supported by the present finding of increased activation in oocytes grown in AO_{10PA}. This correlation reinforces the notion that chromatin remodeling is intricately linked to oocyte developmental competence and highlights the potential of our system to promote optimal chromatin development and subsequent oocyte functionality. Thus, to assess oocyte developmental functionality accurately, parthenogenetic activation was employed, serving to evaluate the degree of cytoplasmic maturation without introducing the variable associated with fertilization and subsequent male pronucleus remodeling. It is noteworthy that oocytes grown long-term on the PCL-patterned scaffold have surpassed the 8-cell block, indicating successful developmental progression. The criticality of surpassing this block is explained by the need for successful embryonic development to proceed beyond the early cleavage stages. Therefore, it is crucial to ensure that oocytes exhibit robust developmental potential beyond this stage. Hence, emphasizing that in the absence of fertilization within a simplified activation model, the cytoplasm of oocytes isolated from differentiated EA follicles in a long-term 3D system on a PCL scaffold behaves similarly to those isolated from SA follicles.

Leveraging a highly biocompatible and FDA-approved material fabricated through electrospinning technology, reproductive medicine may have a substantial leap toward the implementation of either of the strategies based on the use of artificial ovary [51, 52] or the protocols of PA *iv*F applied to different species (in small mammals, such as rodents [96–98], medium-large sized mammals such as sheep [10, 64, 65, 68, 99], goats [100], cows [101, 102], mares [103], pigs [8] and non-human primates [104, 105]).

The use of PCL-based scaffolds may have far-reaching implications for reproductive medicine and fertility preservation, particularly opening innovative strategies for oncological [71, 106] and premature ovarian failure challenges [107]. Furthermore, enhancing the regenerative potential of these scaffolds through surface functionalization with ECM-derived bioactive components represents a forward-looking approach, aimed at improving cellular interactions and promoting the attachment and growth of ovarian follicles in a manner that closely resembles the natural tissue environment [22, 108]. Mimicking the natural ovarian ECM enhances the microenvironmental cues necessary for follicle development, potentially leading to improved follicle health and developmental outcomes [109]. Moreover, tailoring the composition of ECM bioactive components on the PCL-scaffold surface could allow for the customization of the artificial ovary microenvironment based on individual patient characteristics or specific clinical needs.

But not to be outdone, the availability of ovarian-inspired matrices enabling a 3D system for long-term follicle/oocyte development is a unique opportunity to elucidate the fundamental molecular and cellular mechanisms governing fertility.

Conclusions

The study showcased the proof of concept for a next-generation ART use of PCL-patterned scaffold aimed to generate transplantable artificial ovary engrafted with autologous early-stage follicles or to advance *iv*F technologies. Patterned electrospun PCL scaffolds confirmed to be structured for reproducing a three-dimensional bioinspired matrix enabling in vitro the long-term process of multiple PA follicle development. The PCL-based REPROTEN approach may provide, indeed, great potential in advancing *iv*F protocols applied to early stages of follicle recruitment, genetic vulnerability, medications, environmental exposures and toxicities, aging, nutrition, and diseases. At the same time, the present results document through solid functional evidence that the patterned electrospun fibrous scaffolds fabricated with PCL is ready to be moved toward clinical practice for the benefit of people worldwide facing fertility-related challenges.

Abbreviations

ARTs	Assisted Reproductive Technologies
CAD	Computer-Aided Design
CYP11A1	Cytochrome P450 Family 11 Subfamily A Member 1
CYP17A1	Cytochrome P450 Family 17 Subfamily A Member 1
CYP19A1	Cytochrome P450 Family 19 Subfamily A Member 1
EA	Early Antral
eCG	equine Chorionic Gonadotropin
ECM	Extracellular Matrix
FDA	Food and Drug Administration
GV	Germinal Vesicle
GVBD/MI	Germinal Vesicle Break Down/Metaphase 1
hCG	human Chorionic Gonadotropin
IVC	in vitro embryo culture
IVF	in vitro fertilization
ivF	in vitro Folliculogenesis
IVM	in vitro maturation
MII	Metaphase 2
NSN	Non-Surrounding Nucleolus

PA	Preantral
PCL	Poly(ε-caprolactone)
REPROTEN	REPROductive Tissue ENgineering
SN	Surrounding Nucleolus
SNE	Surrounding Nuclear Envelope

Acknowledgements
The authors thank the European Union—Next Generation EU. Project Code: ECS00000041; Project CUP: C43C22000380007; Project Title: Innovation, digitalization, and sustainability for the diffused economy in Central Italy—VITALITY. The authors also thank Fabiana Verni for her valuable contribution in retrieving and transporting the biological material.

Author contributions
B.B. and L.L. made substantial contributions to the conception and design of the work. B.B. and C.D.B. were the major contributors to writing the manuscript. B.B., A.P., L.L., V.R., P.B., A.R.B., I.U., A-ID-B assisted in manuscript preparation and reviewed the manuscript. C.D.B., C.C.S.R., G.C. performed most experiments and B.B., C.D.B., A.P. interpreted the data. C.D.B., A.P., C.C.S.R. analyzed the data and prepared the figures and manuscript draft. L.L., I.U., A-ID-B carried out additional experiments, A.R.B. provided resources. All authors read and approved the final manuscript.

Funding
This research was funded by the European Union—Next Generation EU. Project Code: ECS00000041; Project CUP: C43C22000380007; Project Title: Innovation, digitalization, and sustainability for the diffused economy in Central Italy—VITALITY.

Data availability
No datasets were generated or analysed during the current study.

Declarations

Ethics approval and consent to participate
No ethical issues are encountered in the present research, as all biological materials were obtained from tissues of animals in the food chain discarded by the local slaughterhouse.

Consent for publication
Not applicable.

Competing interests
The authors declare no competing interests.

Author details
[1]Department of Bioscience and Technology for Food, Agriculture and Environment, University of Teramo, 64100 Teramo, Italy
[2]Institute of Biomaterials, Department of Materials Science and Engineering, University of Erlangen–Nuremberg, Cauerstraße 6, 91058 Erlangen, Germany
[3]DGS SpA, Via Paolo di Dono 73, 00142 Rome, Italy

Received: 14 March 2024 / Accepted: 24 July 2024
Published online: 02 August 2024

References

1. Van Montfoort APA, Hanssen LLP, De Sutter P, Viville S, Geraedts JPM, De Boer P. Assisted reproduction treatment and epigenetic inheritance. Hum Reprod Update [Internet]. 2012 [cited 2024 Feb 26];18:171–97. https://pubmed.ncbi.nlm.nih.gov/22267841/.
2. Sjunnesson Y. In vitro fertilisation in domestic mammals—a brief overview. Ups J Med Sci [Internet]. 2020 [cited 2022 Nov 4];125:68. https://www.pmc/articles/PMC7721027/.
3. Heiligentag M, Eichenlaub-Ritter U. Preantral follicle culture and oocyte quality. Reprod Fertil Dev [Internet]. 2017 [cited 2024 Feb 26];30:18–43. https://pubmed.ncbi.nlm.nih.gov/29539300/.
4. Takae S, Suzuki N. Current state and future possibilities of ovarian tissue transplantation. Reprod Med Biol [Internet]. 2019 [cited 2022 Nov 8];18:217–24. https://pubmed.ncbi.nlm.nih.gov/31312099/.
5. Labrune E, Salle B, Lornage J. An Update on In Vitro Folliculogenesis: A New Technique for Post-Cancer Fertility. Biomedicines [Internet]. 2022 [cited 2022 Nov 8];10. https://pubmed.ncbi.nlm.nih.gov/36140316/.
6. O'Brien MJ, Pendola JK, Eppig JJ. A revised protocol for in vitro development of mouse oocytes from primordial follicles dramatically improves their developmental competence. Biol Reprod [Internet]. 2003 [cited 2022 Nov 8];68:1682–6. https://pubmed.ncbi.nlm.nih.gov/12606400/.
7. Daniel SAJ, Armstrong DT, Gore-Langton RE. Growth and development of rat oocytes in vitro. Gamete Res [Internet]. 1989 [cited 2022 Nov 5];24:109–21. https://pubmed.ncbi.nlm.nih.gov/2591848/.
8. Wu J, Carrell DT, Wilcox AL. Development of in vitro-matured oocytes from porcine preantral follicles following intracytoplasmic sperm injection. Biol Reprod [Internet]. 2001 [cited 2022 Nov 8];65:1579–85. https://pubmed.ncbi.nlm.nih.gov/11673278/.
9. Gupta PSP, Ramesh HS, Manjunatha BM, Nandi S, Ravindra JP. Production of buffalo embryos using oocytes from in vitro grown preantral follicles. Zygote. 2008;16:57–63.
10. Arunakumari G, Shanmugasundaram N, Rao VH. Development of morulae from the oocytes of cultured sheep preantral follicles. Theriogenology. 2010;74:884–94.
11. Magalhães DM, Duarte ABG, Araújo VR, Brito IR, Soares TG, Lima IMT et al. In vitro production of a caprine embryo from a preantral follicle cultured in media supplemented with growth hormone. Theriogenology. 2011.
12. de Sá NAR, Ferreira ACA, Sousa FGC, Duarte ABG, Paes VM, Cadenas J et al. First pregnancy after in vitro culture of early antral follicles in goats: Positive effects of anethole on follicle development and steroidogenesis. Mol Reprod Dev [Internet]. 2020 [cited 2022 Nov 8];87:966–77. https://pubmed.ncbi.nlm.nih.gov/32761832/.
13. Xiao S, Zhang J, Romero MM, Smith KN, Shea LD, Woodruff TK. In vitro follicle growth supports human oocyte meiotic maturation. Sci Rep. 2015;5:1–5.
14. McLaughlin M, Albertini DF, Wallace WHB, Anderson RA, Telfer EE. Metaphase II oocytes from human unilaminar follicles grown in a multi-step culture system. Mol Hum Reprod [Internet]. 2018 [cited 2022 Nov 8];24:135–42. https://pubmed.ncbi.nlm.nih.gov/29390119/.
15. Xu F, Lawson MS, Bean Y, Ting AY, Pejovic T, De Geest K et al. Matrix-free 3D culture supports human follicular development from the unilaminar to the antral stage in vitro yielding morphologically normal metaphase II oocytes. Hum Reprod [Internet]. 2021 [cited 2022 Nov 8];36:1326–38. https://pubmed.ncbi.nlm.nih.gov/33681988/.
16. Bakhshandeh B, Zarrintaj P, Oftadeh MO, Keramati F, Fouladiha H, Sohrabi-jahromi S et al. Tissue engineering; strategies, tissues, and biomaterials. Biotechnol Genet Eng Rev [Internet]. 2017 [cited 2022 Nov 9];33:144–72. https://pubmed.ncbi.nlm.nih.gov/29385962/.
17. Cho E, Kim YY, Noh K, Ku SY. A new possibility in fertility preservation: The artificial ovary. J Tissue Eng Regen Med [Internet]. 2019 [cited 2024 Jan 27];13:1294–315. https://pubmed.ncbi.nlm.nih.gov/31062444/.
18. Dolmans M-M, Amorim CA. FERTILITY PRESERVATION: Construction and use of artificial ovaries. Reproduction [Internet]. 2019 [cited 2022 Nov 2];158:F15–25. https://rep.bioscientifica.com/view/journals/rep/158/5/REP-18-0536.xml.
19. Xiang D, Zhou E, Wang M, Wang K, Zhou S, Ma Q et al. Artificial ovaries constructed from biodegradable chitin-based hydrogels with the ability to restore ovarian endocrine function and alleviate osteoporosis in ovariectomized mice. Reprod Biol Endocrinol [Internet]. 2023 [cited 2024 May 8];21. https://pubmed.ncbi.nlm.nih.gov/37208699/.
20. Chen J, Torres-de la Roche LA, Kahlert UD, Isachenko V, Huang H, Hennefründ J, et al. Artificial Ovary for Young female breast Cancer patients. Front Med. 2022;9:837022.
21. Zubizarreta ME, Xiao S. Bioengineering models of female reproduction. Bio-Design Manuf [Internet]. 2020 [cited 2024 May 8];3:237–51. https://link.springer.com/article/10.1007/s42242-020-00082-8.
22. Pors SE, Ramløse M, Nikiforov D, Lundsgaard K, Cheng J, Yding Andersen C et al. Initial steps in reconstruction of the human ovary: survival of pre-antral stage follicles in a decellularized human ovarian scaffold. Hum Reprod [Internet]. 2019 [cited 2022 Nov 9];34:1523–35. https://pubmed.ncbi.nlm.nih.gov/31286144/.
23. Healy MW, Dolitsky SN, Villancio-Wolter M, Raghavan M, Tillman AR, Morgan NY et al. Creating an Artificial 3-Dimensional Ovarian Follicle Culture System Using a Microfluidic System. Micromachines [Internet]. 2021 [cited 2024 May 8];12:1–15. https://pubmed.ncbi.nlm.nih.gov/33806282/.

24. West ER, Shea LD, Woodruff TK. Engineering the follicle microenvironment. Semin Reprod Med [Internet]. 2007 [cited 2022 Nov 17];25:287–99. https://pubmed.ncbi.nlm.nih.gov/17594609/.
25. Chiti MC, Donnez J, Amorim CA, Dolmans M-M. From isolation of human ovarian follicles to the artificial ovary: tips and tricks. Minerva Obstet Gynecol [Internet]. 2018 [cited 2024 Feb 15];70. https://www.minervamedica.it/index2.php?show=R09Y2018N04A0444.
26. Kniazeva E, Hardy AN, Boukaidi SA, Woodruff TK, Jeruss JS, Shea LD. Primordial Follicle Transplantation within Designer Biomaterial Grafts Produce Live Births in a Mouse Infertility Model. Sci Rep [Internet]. 2015 [cited 2022 Nov 5];5. https://pubmed.ncbi.nlm.nih.gov/26633657/.
27. Laronda MM, Jakus AE, Whelan KA, Wertheim JA, Shah RN, Woodruff TK. Initiation of puberty in mice following decellularized ovary transplant. Biomaterials [Internet]. 2015 [cited 2022 Nov 9];50:20–9. https://pubmed.ncbi.nlm.nih.gov/25736492/.
28. Amorim CA, Shikanov A. The artificial ovary: current status and future perspectives. Future Oncol [Internet]. 2016 [cited 2022 Nov 10];12:2323–32. https://pubmed.ncbi.nlm.nih.gov/27396310/.
29. Dadashzadeh A, Moghassemi S, Shavandi A, Amorim CA. A review on biomaterials for ovarian tissue engineering. Acta Biomater [Internet]. 2021 [cited 2022 Nov 10];135:48–63. https://pubmed.ncbi.nlm.nih.gov/34454083/.
30. Francés-Herrero E, Lopez R, Hellström M, de Miguel-Gómez L, Herraiz S, Brännström M et al. Bioengineering trends in female reproduction: a systematic review. Hum Reprod Update [Internet]. 2022 [cited 2022 Sep 17]; https://pubmed.ncbi.nlm.nih.gov/35652272/.
31. Soares M, Sahrari K, Amorim CA, Saussoy P, Donnez J, Dolmans MM. Evaluation of a human ovarian follicle isolation technique to obtain disease-free follicle suspensions before safely grafting to cancer patients. Fertil Steril. 2015;104:672–e6802.
32. Hassanpour A, Talaei-Khozani T, Kargar-Abarghouei E, Razban V, Vojdani Z. Decellularized human ovarian scaffold based on a sodium lauryl ester sulfate (SLES)-treated protocol, as a natural three-dimensional scaffold for construction of bioengineered ovaries. Stem Cell Res Ther [Internet]. 2018 [cited 2022 Nov 9];9:252. https://pubmed.ncbi.nlm.nih.gov/30257706/.
33. Vanacker J, Luyckx V, Dolmans MM, Des Rieux A, Jaeger J, Van Langendonckt A et al. Transplantation of an alginate-matrigel matrix containing isolated ovarian cells: first step in developing a biodegradable scaffold to transplant isolated preantral follicles and ovarian cells. Biomaterials [Internet]. 2012 [cited 2022 Nov 9];33:6079–85. https://pubmed.ncbi.nlm.nih.gov/22658800/.
34. Rios PD, Kniazeva E, Lee HC, Xiao S, Oakes RS, Saito E et al. Retrievable hydrogels for ovarian follicle transplantation and oocyte collection. Biotechnol Bioeng [Internet]. 2018 [cited 2024 Jan 27];115:2075–86. https://pubmed.ncbi.nlm.nih.gov/29704433/.
35. Paulini F, Vilela JMV, Chiti MC, Donnez J, Jadoul P, Dolmans MM et al. Survival and growth of human preantral follicles after cryopreservation of ovarian tissue, follicle isolation and short-term xenografting. Reprod Biomed Online [Internet]. 2016 [cited 2022 Nov 9];33:425–32. https://pubmed.ncbi.nlm.nih.gov/27210771/.
36. Smith RM, Shikanov A, Kniazeva E, Ramadurai D, Woodruff TK, Shea LD. Fibrin-mediated delivery of an ovarian follicle pool in a mouse model of infertility. Tissue Eng Part A [Internet]. 2014 [cited 2024 Jan 27];20:3021–30. https://pubmed.ncbi.nlm.nih.gov/24802617/.
37. Luyckx V, Dolmans MM, Vanacker J, Legat C, Fortuño Moya C, Donnez J et al. A new step toward the artificial ovary: survival and proliferation of isolated murine follicles after autologous transplantation in a fibrin scaffold. Fertil Steril [Internet]. 2014 [cited 2022 Nov 10];101:1149–56. https://pubmed.ncbi.nlm.nih.gov/24462059/.
38. Kim J, Perez AS, Claflin J, David A, Zhou H, Shikanov A. Synthetic hydrogel supports the function and regeneration of artificial ovarian tissue in mice. NPJ Regen Med [Internet]. 2016 [cited 2024 Jan 27];1. https://pubmed.ncbi.nlm.nih.gov/28856012/.
39. Laronda MM, Rutz AL, Xiao S, Whelan KA, Duncan FE, Roth EW et al. A bioprosthetic ovary created using 3D printed microporous scaffolds restores ovarian function in sterilized mice. Nat Commun [Internet]. 2017 [cited 2022 Nov 9];8. https://pubmed.ncbi.nlm.nih.gov/28509899/.
40. Nikolova MP, Chavali MS. Recent advances in biomaterials for 3D scaffolds: A review. Bioact Mater [Internet]. 2019 [cited 2024 May 8];4:271–92. https://pubmed.ncbi.nlm.nih.gov/31709311/.
41. Do AV, Khorsand B, Geary SM, Salem AK. 3D Printing of Scaffolds for Tissue Regeneration Applications. Adv Healthc Mater [Internet]. 2015 [cited 2024 May 8];4:1742–62. https://pubmed.ncbi.nlm.nih.gov/26097108/.
42. Liu N, Zhang X, Guo Q, Wu T, Wang Y. 3D Bioprinted scaffolds for tissue repair and regeneration. Front Mater. 2022;9:925321.
43. Tamay DG, Usal TD, Alagoz AS, Yucel D, Hasirci N, Hasirci V. 3D and 4D Printing of Polymers for Tissue Engineering Applications. Front Bioeng Biotechnol [Internet]. 2019 [cited 2024 Feb 26];7:164. https://www.pmc/articles/PMC6629835/.
44. Hu C, Zhang W, Li P. 3D Printing and Its Current Status of Application in Obstetrics and Gynecological Diseases. Bioeng (Basel, Switzerland) [Internet]. 2023 [cited 2024 May 8];10. https://pubmed.ncbi.nlm.nih.gov/36978690/.
45. Wu T, Gao YY, Su J, Tang XN, Chen Q, Ma LW et al. Three-dimensional bioprinting of artificial ovaries by an extrusion-based method using gelatin-methacryloyl bioink. Climacteric [Internet]. 2022 [cited 2024 May 8];25:170–8. https://pubmed.ncbi.nlm.nih.gov/33993814/.
46. R G AP SS, Bajaj G, John AE, Chandran S, Kumar VV et al. A review on the recent applications of synthetic biopolymers in 3D printing for biomedical applications. J Mater Sci Mater Med [Internet]. 2023 [cited 2024 May 8];34. https://pubmed.ncbi.nlm.nih.gov/37982917/.
47. Ferronato G, de Vit A, Silveira FF. JC da. 3D culture applied to reproduction in females: possibilities and perspectives. Anim Reprod [Internet]. 2024 [cited 2024 May 8];21. https://pubmed.ncbi.nlm.nih.gov/38510565/.
48. Woods I, Flanagan TC. Electrospinning of biomimetic scaffolds for tissue-engineered vascular grafts: threading the path. Expert Rev Cardiovasc Ther [Internet]. 2014 [cited 2024 Feb 26];12:815–32. https://pubmed.ncbi.nlm.nih.gov/24903895/.
49. Parham S, Kharazi AZ, Bakhsheshi-Rad HR, Ghayour H, Ismail AF, Nur H et al. Electrospun Nano-Fibers for Biomedical and Tissue Engineering Applications: A Comprehensive Review. Mater (Basel, Switzerland) [Internet]. 2020 [cited 2024 Feb 26];13. https://pubmed.ncbi.nlm.nih.gov/32384813/.
50. Gargus ES, Rogers HB, McKinnon KE, Edmonds ME, Woodruff TK. Engineered reproductive tissues. Nat Biomed Eng [Internet]. 2020 [cited 2024 Feb 26];4:381–93. https://pubmed.ncbi.nlm.nih.gov/32251392/.
51. Raffel N, Dittrich R, Bäuerle T, Seyler L, Fattahi A, Hoffmann I et al. Novel approach for the assessment of ovarian follicles infiltration in polymeric electrospun patterned scaffolds. PLoS One [Internet]. 2019 [cited 2022 Nov 9];14:e0215985. https://journals.plos.org/plosone/article?id=10.1371/journal.pone.0215985.
52. Liverani L, Raffel N, Fattahi A, Preis A, Hoffmann I, Boccaccini AR et al. Electrospun patterned porous scaffolds for the support of ovarian follicles growth: a feasibility study. Sci Rep [Internet]. 2019 [cited 2022 Oct 5];9. https://pubmed.ncbi.nlm.nih.gov/30718584/.
53. Tamadon A, Park KH, Kim YY, Kang BC, Ku SY. Efficient biomaterials for tissue engineering of female reproductive organs. Tissue Eng Regen Med [Internet]. 2016 [cited 2022 Nov 9];13:447–54. https://pubmed.ncbi.nlm.nih.gov/30603426/.
54. Fattahi A, Liverani L, Dittrich R, Hoffmann I, Boccaccini AR, Beckmann MW et al. Optimization of Porcine Ovarian Follicle Isolation Methods for Better Developmental Potential. Tissue Eng Part A [Internet]. 2020 [cited 2022 Nov 9];26:712–9. https://pubmed.ncbi.nlm.nih.gov/32598233/.
55. Liverani L, Guarino V, La Carrubba V, Boccaccini AR. Porous biomaterials and scaffolds for tissue engineering. Encycl Biomed Eng [Internet]. 2017 [cited 2022 Nov 9];1–3:188–202. https://iris.unipa.it/handle/10447/463930.
56. Di Berardino C, Liverani L, Peserico A, Capacchietti G, Russo V, Bernabò N et al. When Electrospun Fiber Support Matters: In Vitro Ovine Long-Term Folliculogenesis on Poly (Epsilon Caprolactone) (PCL)-Patterned Fibers. Cells [Internet]. 2022 [cited 2022 Oct 5];11. https://pubmed.ncbi.nlm.nih.gov/35741097/.
57. Bernabò N, Di Berardino C, Capacchietti G, Peserico A, Buoncuore G, Tosi U et al. In Vitro Folliculogenesis in Mammalian Models: A Computational Biology Study. Front Mol Biosci [Internet]. 2021 [cited 2022 Oct 5];8. https://pubmed.ncbi.nlm.nih.gov/34859047/.
58. Peserico A, Di Berardino C, Capacchietti G, Camerano Spelta Rapini C, Liverani L, Boccaccini AR et al. IVM advances for early antral follicle-enclosed oocytes Coupling Reproductive tissue Engineering to Inductive Influences of Human Chorionic Gonadotropin and Ovarian Surface Epithelium Coculture. Int J Mol Sci [Internet]. 2023 [cited 2024 Jan 19];24. Available from: /pmc/articles/PMC10095509/.
59. Tiyek I, Gunduz A, Yalcinkaya F, Chaloupek J. Influence of Electrospinning Parameters on the Hydrophilicity of Electrospun Polycaprolactone Nanofibres. J Nanosci Nanotechnol [Internet]. 2019 [cited 2024 May 13];19:7251–60. https://pubmed.ncbi.nlm.nih.gov/31039883/.
60. Qin X, Wu D. Effect of different solvents on poly(caprolactone)(PCL) electrospun nonwoven membranes. J Therm Anal Calorim [Internet]. 2012

[cited 2024 May 13];107:1007–13. https://link.springer.com/article/10.1007/s10973-011-1640-4.
61. Ferreira JL, Gomes S, Henriques C, Borges JP, Silva JC. Electrospinning polycaprolactone dissolved in glacial acetic acid: Fiber production, nonwoven characterization, and In Vitro evaluation. J Appl Polym Sci [Internet]. 2014 [cited 2024 May 13];131. https://onlinelibrary.wiley.com/doi/full/https://doi.org/10.1002/app.41068.
62. Liverani L, Boccaccini AR. Versatile Production of Poly(Epsilon-Caprolactone) Fibers by Electrospinning Using Benign Solvents. Nanomater (Basel, Switzerland) [Internet]. 2016 [cited 2022 Nov 9];6. https://pubmed.ncbi.nlm.nih.gov/28335202/.
63. Unalan I, Slavik B, Buettner A, Goldmann WH, Frank G, Boccaccini AR. Physical and Antibacterial Properties of Peppermint Essential Oil loaded poly (ε-caprolactone) (PCL) Electrospun Fiber Mats for Wound Healing. Front Bioeng Biotechnol. 2019;7:488792.
64. Di Berardino C, Peserico A, Capacchietti G, Crociati M, Monaci M, Tosi U et al. Equine chorionic gonadotropin as an effective fsh replacement for in vitro ovine follicle and oocyte development. Int J Mol Sci. 2021;22.
65. Cecconi S, Barboni B, Coccia M, Mattioli M. In vitro development of sheep preantral follicles. Biol Reprod. 1999.
66. Newton H, Picton H, Gosden RG. In vitro growth of oocyte-granulosa cell complexes isolated from cryopreserved ovine tissue. J Reprod Fertil [Internet]. 1999 [cited 2022 Nov 8];115:141–50. https://pubmed.ncbi.nlm.nih.gov/10341732/.
67. Cecconi S, Capacchietti G, Russo V, Berardinelli P, Mattioli M, Barboni B. In Vitro Growth of Preantral Follicles Isolated from Cryopreserved Ovine Ovarian Tissue. Biol Reprod [Internet]. 2004 [cited 2022 Nov 9];70:12–7. http://www.biolreprod.org.
68. Barboni B, Russo V, Cecconi S, Curini V, Colosimo A, Garofalo MLA et al. In Vitro grown sheep preantral follicles yield oocytes with normal nuclear-epigenetic maturation. PLoS ONE. 2011;6.
69. Amorim CA. Special Issue Devoted to a New Field of Regenerative Medicine: Reproductive Tissue Engineering. Ann Biomed Eng [Internet]. 2017 [cited 2022 Nov 9];45:1589–91. https://pubmed.ncbi.nlm.nih.gov/28567657/.
70. Masciangelo R, Bosisio C, Donnez J, Amorim CA, Dolmans MM. Safety of ovarian tissue transplantation in patients with borderline ovarian tumors. Hum Reprod [Internet]. 2018 [cited 2022 Nov 8];33:212–9. https://pubmed.ncbi.nlm.nih.gov/29281007/.
71. Fisch B, Abir R. Female fertility preservation: past, present and future. Reproduction. 2018;156:F11–27.
72. Wang X, Wu D, Li W, Yang L. Emerging biomaterials for reproductive medicine. Eng Regen. 2021;2:230–45.
73. Xu M, Kreeger PK, Shea LD, Woodruff TK. Tissue-engineered follicles produce live, fertile offspring. Tissue Eng [Internet]. 2006 [cited 2022 Nov 7];12:2739–46. https://pubmed.ncbi.nlm.nih.gov/17518643/.
74. Kim YB, Kim GH. PCL/alginate composite scaffolds for hard tissue engineering: fabrication, characterization, and cellular activities. ACS Comb Sci [Internet]. 2015 [cited 2022 Nov 9];17:87–99. https://pubmed.ncbi.nlm.nih.gov/25541639/.
75. Zhu Y, Wan Y, Zhang J, Yin D, Cheng W. Manufacture of layered collagen/chitosan-polycaprolactone scaffolds with biomimetic microarchitecture. Colloids Surf B Biointerfaces. 2014;113:352–60.
76. Cui Z, Wright LD, Guzzo R, Freeman JW, Drissi H, Nair LS. Poly(d-lactide)/poly(caprolactone) nanofiber-thermogelling chitosan gel composite scaffolds for osteochondral tissue regeneration in a rat model. http://dx.doi.org/101177/0883911512472278 [Internet]. 2013 [cited 2024 Jan 27];28:115–25. https://doi.org/10.1177/0883911512472278.
77. Firoozi N, Rezayan AH, Tabatabaei Rezaei SJ, Mir-Derikvand M, Nabid MR, Nourmohammadi J et al. Synthesis of poly(ε-caprolactone)-based polyurethane semi-interpenetrating polymer networks as scaffolds for skin tissue regeneration. http://dx.doi.org/101080/009140372016161276059 [Internet]. 2017 [cited 2022 Nov 9];66:805–11. https://www.tandfonline.com/doi/abs/https://doi.org/10.1080/00914037.2016.1276059.
78. Bolaina-Lorenzo E, Martinez-Ramos C, Monleón-Pradas M, Herrera-Kao W, Cauich-Rodriguez JV, Cervantes-Uc JM. Electrospun polycaprolactone/chitosan scaffolds for nerve tissue engineering: physicochemical characterization and Schwann cell biocompatibility. Biomed Mater [Internet]. 2016 [cited 2022 Nov 9];12. https://pubmed.ncbi.nlm.nih.gov/27934786/.
79. Park JH, Lee BK, Park SH, Kim MG, Lee JW, Lee HY et al. Preparation of Biodegradable and Elastic Poly(ε-caprolactone-co-lactide) Copolymers and evaluation as a localized and sustained drug delivery carrier. Int J Mol Sci [Internet]. 2017 [cited 2024 Feb 26];18. Available from: /pmc/articles/PMC5372682/.
80. Chu B, Zhang L, Qu Y, Chen X, Peng J, Huang Y et al. Synthesis, characterization and drug loading property of Monomethoxy-Poly(ethylene glycol)-Poly(ε-caprolactone)-Poly(D,L-lactide) (MPEG-PCLA) copolymers. Sci Reports 2016 61 [Internet]. 2016 [cited 2024 Feb 26];6:1–15. https://www.nature.com/articles/srep34069.
81. Simon LE, Rajendra Kumar T, Duncan FE. In vitro ovarian follicle growth: a comprehensive analysis of key protocol variables†. Biol Reprod [Internet]. 2020 [cited 2022 Nov 17];103:455–70. https://pubmed.ncbi.nlm.nih.gov/32406908/.
82. Casarini L, Riccetti L, De Pascali F, Gilioli L, Marino M, Vecchi E et al. Estrogen Modulates Specific Life and Death Signals Induced by LH and hCG in Human Primary Granulosa Cells In Vitro. Int J Mol Sci [Internet]. 2017 [cited 2023 Feb 19];18. https://pubmed.ncbi.nlm.nih.gov/28452938/.
83. Parrish EM, Siletz A, Xu M, Woodruff TK, Shea LD. Gene expression in mouse ovarian follicle development in vivo versus an ex vivo alginate culture system. Reproduction [Internet]. 2011 [cited 2022 Nov 17];142:309–18. https://pubmed.ncbi.nlm.nih.gov/21610168/.
84. Heidarzadehpilehrood R, Pirhoushiaran M, Abdollahzadeh R, Osman MB, Sakinah M, Nordin N et al. A Review on CYP11A1, CYP17A1, and CYP19A1 Polymorphism Studies: Candidate Susceptibility Genes for Polycystic Ovary Syndrome (PCOS) and Infertility. Genes (Basel) [Internet]. 2022 [cited 2022 Nov 10];13. https://pubmed.ncbi.nlm.nih.gov/35205347/.
85. Seamark RF, Hamilton RP, Moor RM, Proceedings. Changes in the sterol content of sheep ovarian follicles in culture: relationship to steroidogenesis and effects of gonadotrophins. J Reprod Fertil [Internet]. 1976 [cited 2023 Jan 9];46:521. https://pubmed.ncbi.nlm.nih.gov/1255616/.
86. Zheng M, Andersen CY, Rasmussen FR, Cadenas J, Christensen ST, Mamsen LS. Expression of genes and enzymes involved in ovarian steroidogenesis in relation to human follicular development. Front Endocrinol (Lausanne) [Internet]. 2023 [cited 2024 Feb 16];14. https://pubmed.ncbi.nlm.nih.gov/37964966/.
87. Russo V, Martelli A, Berardinelli P, Di Giacinto O, Bernabò N, Fantasia D et al. Modifications in chromatin morphology and organization during sheep oogenesis. Microsc Res Tech [Internet]. 2007 [cited 2023 Feb 19];70:733–44. https://pubmed.ncbi.nlm.nih.gov/17394198/.
88. Eppig JJ. Development in vitro of mouse oocytes from primordial follicles. Biol Reprod. 1996;54:197–207.
89. Yeste M, Jones C, Amdani SN, Patel S, Coward K. Oocyte activation deficiency: a role for an oocyte contribution? Hum Reprod Update [Internet]. 2016 [cited 2023 Feb 19];22:23–47. https://pubmed.ncbi.nlm.nih.gov/26346057/.
90. Neri QV, Lee B, Rosenwaks Z, Machaca K, Palermo GD. Understanding fertilization through intracytoplasmic sperm injection (ICSI). Cell Calcium [Internet]. 2014 [cited 2023 Feb 19];55:24–37. https://pubmed.ncbi.nlm.nih.gov/24290744/.
91. Zuccotti M, Garagna S, Merico V, Monti M, Redi CA. Chromatin organisation and nuclear architecture in growing mouse oocytes. Mol Cell Endocrinol [Internet]. 2005 [cited 2023 Feb 19];234:11–7. https://pubmed.ncbi.nlm.nih.gov/15836948/.
92. Luciano AM, Franciosi F, Modina SC, Lodde V. Gap junction-mediated communications regulate chromatin remodeling during bovine oocyte growth and differentiation through cAMP-dependent mechanism(s). Biol Reprod [Internet]. 2011 [cited 2024 Feb 28];85:1252–9. https://pubmed.ncbi.nlm.nih.gov/21816847/.
93. Franciosi F, Coticchio G, Lodde V, Tessaro I, Modina SC, Fadini R et al. Natriuretic peptide precursor C delays meiotic resumption and sustains gap junction-mediated communication in bovine cumulus-enclosed oocytes. Biol Reprod [Internet]. 2014 [cited 2022 Nov 7];91. https://pubmed.ncbi.nlm.nih.gov/25078681/.
94. Sugimura S, Ritter LJ, Sutton-McDowall ML, Mottershead DG, Thompson JG, Gilchrist RB. Amphiregulin co-operates with bone morphogenetic protein 15 to increase bovine oocyte developmental competence: effects on gap junction-mediated metabolite supply. Mol Hum Reprod [Internet]. 2014 [cited 2022 Nov 7];20:499–513. https://pubmed.ncbi.nlm.nih.gov/24557840/.
95. Santiquet NW, Greene AF, Becker J, Barfield JP, Schoolcraft WB, Krisher RL. A pre-in vitro maturation medium containing cumulus oocyte complex ligand-receptor signaling molecules maintains meiotic arrest, supports the cumulus oocyte complex and improves oocyte developmental competence. Mol Hum Reprod [Internet]. 2017 [cited 2024 Feb 28];23:594–606. https://pubmed.ncbi.nlm.nih.gov/28586460/.
96. Tanaka Y, Matsuzaki T, Tanaka N, Iwasa T, Kuwahara A, Irahara M. Activin effects on follicular growth in in vitro preantral follicle culture. J Med Invest

[Internet]. 2019 [cited 2024 Feb 28];66:165–71. https://pubmed.ncbi.nlm.nih.gov/31064932/.
97. Kim KC, Park MH, Yun JI, Lim JM, Lee ST. The native form of follicle-stimulating hormone is essential for the growth of mouse preantral follicles in vitro. Reprod Biol [Internet]. 2021 [cited 2024 Feb 28];21. https://pubmed.ncbi.nlm.nih.gov/34144372/.
98. Rajabi Z, Yazdekhasti H, Noori Mugahi SMH, Abbasi M, Kazemnejad S, Shirazi A et al. Mouse preantral follicle growth in 3D co-culture system using human menstrual blood mesenchymal stem cell. Reprod Biol [Internet]. 2018 [cited 2024 Feb 28];18:122–31. https://pubmed.ncbi.nlm.nih.gov/29454805/.
99. Barros VRP, Monte APO, Lins TLBG, Santos JM, Menezes VG, Cavalcante AYP et al. In vitro survival, growth, and maturation of sheep oocytes from secondary follicles cultured in serum-free conditions: impact of a constant or a sequential medium containing recombinant human FSH. Domest Anim Endocrinol. 2019.
100. Magalhães DM, Duarte ABG, Araújo VR, Brito IR, Soares TG, Lima IMT et al. In vitro production of a caprine embryo from a preantral follicle cultured in media supplemented with growth hormone. Theriogenology [Internet]. 2011 [cited 2022 Nov 8];75:182–8. https://pubmed.ncbi.nlm.nih.gov/20875671/.
101. Nuttinck F, Mermillod P, Massip A, Dessy F. Characterization of in vitro growth of bovine preantral ovarian follicles: A preliminary study. Theriogenology [Internet]. 1993 [cited 2022 Nov 8];39:811–21. https://pubmed.ncbi.nlm.nih.gov/16727255/.
102. Saha S, Shimizu M, Geshi M, Izaike Y. In vitro culture of bovine preantral follicles. Anim Reprod Sci [Internet]. 2000 [cited 2022 Nov 8];63:27–39. https://pubmed.ncbi.nlm.nih.gov/10967238/.
103. Max MC, Bizarro-Silva C, Búfalo I, González SM, Lindquist AG, Gomes RG et al. In vitro culture supplementation of EGF for improving the survival of equine preantral follicles. In Vitro Cell Dev Biol Anim [Internet]. 2018 [cited 2024 Feb 28];54:687–91. https://pubmed.ncbi.nlm.nih.gov/30284096/.
104. Xu M, West-Farrell ER, Stouffer RL, Shea LD, Woodruff TK, Zelinski MB. Encapsulated three-Dimensional Culture supports Development of Nonhuman Primate secondary Follicles1. Biol Reprod. 2009;81:587–94.
105. Xu J, Lawson MS, Yeoman RR, Pau KY, Barrett SL, Zelinski MB et al. Secondary follicle growth and oocyte maturation during encapsulated three-dimensional culture in rhesus monkeys: effects of gonadotrophins, oxygen and fetuin. Hum Reprod [Internet]. 2011 [cited 2022 Nov 17];26:1061–72. https://pubmed.ncbi.nlm.nih.gov/21362681/.
106. Roness H, Meirow D, FERTILITY PRESERVATION. Follicle reserve loss in ovarian tissue transplantation. Reproduction [Internet]. 2019 [cited 2022 Nov 8];158:F35–44. https://pubmed.ncbi.nlm.nih.gov/31394506/.
107. Condorelli M, Demeestere I. Challenges of fertility preservation in non-oncological diseases. Acta Obstet Gynecol Scand [Internet]. 2019 [cited 2024 Mar 4];98:638–46. https://onlinelibrary.wiley.com/doi/full/10.1111/aogs.13577.
108. Rijal G. The decellularized extracellular matrix in regenerative medicine. https://doi.org/102217/rme-2017-0046 [Internet]. 2017 [cited 2022 Nov 9];12:475–7. https://www.futuremedicine.com/doi/https://doi.org/10.2217/rme-2017-0046.
109. Tagler D, Makanji Y, Tu T, Bernabé BP, Lee R, Zhu J et al. Promoting extracellular matrix remodeling via ascorbic acid enhances the survival of primary ovarian follicles encapsulated in alginate hydrogels. Biotechnol Bioeng [Internet]. 2014 [cited 2022 Nov 8];111:1417–29. https://pubmed.ncbi.nlm.nih.gov/24375265/.

Publisher's Note